1968

Measurement of dynamic kc from the drop weight tear test, August 1968 (Luft's M.S. thesis)

David E. Luft

Ronald B. Madison

G. R. Irwin

MEASUREMENT OF DYNAMIC K_C FROM THE DROP WEIGHT TEAR TEST

by

David E. Luft

Ronald B. Madison

G. R. Irwin

Fritz Engineering Laboratory
Department of Civil Engineering
Lehigh University
Bethlehem, Pennsylvania

August 1968

Fritz Engineering Laboratory Report No. 335.1

TABLE OF CONTENTS

TABLE OF CONTENTS (continued)

LIST OF TABLES

LIST OF FIGURES

LIST OF FIGURES (continued)

ABSTRACT

This investigation deals with the measurement of the dynamic fracture toughness of ASTM Grade A441 bridge steel, a rate sensitive material, using a specially built drop weight tear testing machine.

Preliminary tests involved developing a reliable testing procedure whereby dynamic K_C could be measured using a quasi-static linear elastic stress solution. Variables in this series of preliminary tests involved a pressed notch versus a fatigue crack, the influence of drop height, and different types of loading pads.

Dynamic fracture tests were carried out on 1/2 inch plate at different temperatures ranging from -100° F to $+ 30^{\circ}$ F. Electric resistance gages on the specimens were used to measure surface crack speed and specimen response during the loading cycle.

A compliance calibration was carried out on a three-point-bend aluminum model, twice the size of its steel prototype, in order to determine the relationship between the stress intensity factor (K) and the crack length (a).

Fracture toughness values, K_C and K_{IC}, are presented as a function of temperature for the 1/2 inch plate. The agreement of an estimate of K_{IC} (dynamic) from the dynamic yield strength at the NDT shows that the strain rate developed in the drop weight test gives K_{IC} values within 10% of those for a running crack.

1. INTRODUCTION

1.1 Scope and Purpose

Toughness measurements based on the theory of linear elastic Fracture Mechanics are usually obtained from static tests as outlined in the ASTM publication "Plane Strain Crack Toughness Testing".[1]

The purpose of this investigation was to obtain a reliable method whereby a dynamic fracture toughness (K_C) could be measured using an instrumented drop weight tear test.

The material being tested was a low carbon steel, ASTM Grade A441, "High Strength Low Alloy Structural Manganese Vanadium Steel" with a yield strength of 60 ksi.[2] This steel is rate sensitive to dynamic loading, that is, the yield strength is increased by an increase of strain rate.

1.2 Historical Background

Dynamic fracture toughness testing with Charpy V and Charpy keyhole notch specimens was developed during the 1910-1945 period.[3] These tests provided a rough but quantitative means of relating fracture energy to specimen temperature with specimens of different notch sharpness. The first natural crack test was a drop weight test of a specimen containing a brittle weld flaw. This was used for the determination of a "nil-ductility" transition temperature (NDTT).[4]

Subsequently drop weight tear tests were developed by the Naval Research Laboratory[5] and the Battelle Memorial Institute[6] primarily to observe the response of plate materials to a fast running crack. Such tests were used to establish the temperature region of plane-strain to mixed-mode or plane stress transition for rate sensitive steels, 1 inch or less in thickness and yield strengths below 100 ksi. Since 1960 the Naval Research Laboratory has used similar test methods to study fracture toughness of high strength steels, non-ferrous metals such as titanium and aluminum alloys, and low strength steels in the form of heavy plate thicknesses.

Since 1953 research in the crack and stress conditions which determine the initiation and propagation of fracture was directed along two separate paths, that of linear elastic fracture mechanics and dynamic crack testing. Fracture Mechanics, based on Griffith's[7] energy analysis and later modified by Irwin[8] and Orowan,[9] is a mathematical treatment of the elastic stress field conditions at crack tips. It relates stress level at fracture to flaw size using the parameters, K_C and K_{IC}. Dynamic crack tests involve measuring the strain to fracture, or energy to fracture of relatively simple specimens. The Robertson Crack-Arrest Test, the Drop Weight NDT Test, and the Drop Weight Tear Test fall in this category.

Actual instrumentation of a drop weight machine for the purpose of applying the analysis methods of Fracture Mechanics was not carried out until recently. At United States Steel Corporation, Shoemaker and Rolfe have used an instrumented specimen to monitor the load rather

than an instrumented impacting load cell.[10] By doing so they have eliminated the problems of dynamic response of the specimen and inertial forces.

1.3 General Review of the Problem

Krafft and Irwin[11] found that rate sensitive steels exhibit a K_{IC} versus crack tip stress rate relationship as shown in Fig. 1. To obtain the minimum K_{IC} value, a dynamic test is needed to induce a high strain rate in the specimen. For this reason it was decided to instrument a specially built drop weight tear testing machine for determining the minimum fracture toughness of a typical bridge steel, ASTM Grade A441.

The general difficulty with dynamic testing using an instrumented load cell is the inertia forces involved. These become more serious with increase of specimen size. On the other hand, for the purpose of K_{IC} testing, the specimen dimensions must be large compared to the plastic zone size to produce plane strain conditions at the leading edge of the crack. Due to the ductile nature of low carbon steel, the plastic zone is large. This forces the experimenter to use unusually thick specimens and these, in turn, cause greater inertia forces.

Other problems involved are the determination of the dynamic yield strength of the material, the dynamic response of the specimen at the moment of crack initiation, and the influences of specimen shape and size. All of these factors influence the fracture toughness computations.

1.4 Test Program

The primary test program involved developing the instrumentation for a drop weight machine and a testing method whereby it was felt that a quasi-static analysis could be used for K_C and K_{IC} determination. Twenty-five dynamic toughness tests were conducted on 1/2 inch thick ASTM Grade A441 steel plate at various temperatures ranging from -100° F to $+30^{\circ}$ F.

To verify the K value computational procedure, a compliance calibration was carried out on an aluminum model twice the size of its steel prototype.

Additional tension tests were conducted to determine the plastic yield properties of the material in relation to strain rate.

2. TEST SPECIMENS

2.1 Specimen Material

All fracture specimens were cut from commercially rolled plate, a manganese vanadium silicon killed steel of ASTM Grade A441. No controlled rolling or normalizing took place since a material typical of the class used for bridges was desired. All plates were rolled from three consecutive ingots of the same heat on the 60-inch Universal mill at the Sparrows Point plant of Bethlehem Steel Corporation to four desired thicknesses: 1/2, 1, 1-1/2, and 2 inches. Reference to Table 1 gives both the chemical properties of all plate thicknesses and the mechanical properties of the 1/2 inch plate.

The 1/2 inch plate was found to have a 50% FATT (fracture appearance transition temperature) of 80° F as indicated by the drop weight tear data in Fig. 2. This data was obtained using the Battelle DWTT testing procedure from an industrial drop weight machine at Homer Research Laboratories of Bethlehem Steel Corporation.

Charpy data, which is shown in Fig. 3, was obtained both from specimens oriented parallel to the rolling direction and perpendicular to the rolling direction.

2.2 Specimen Geometry

Fracture specimens were 12" long, 3" deep, and 1/2" thick. Each 6' by 3' plate yielded 72 specimens as shown in Fig. 4, half cut with the rolling direction parallel to the direction of crack propagation, hereafter referred to as transverse specimens, and half with the rolling direction perpendicular to the direction of crack propagation, hereafter referred to as longitudinal specimens.

2.3 Specimen Preparation

With the possibility of correlating the results of the instrumented machine to the commercial drop weight test, preliminary tests were carried out using specimens that contained a pressed notch 0.16 in. deep. Subsequently, to apply the theory of linear elastic fracture mechanics, it was decided that all test specimens would contain a 3/4 in. deep starting crack introduced by fatigue.

To facilitate the growth of a fatigue crack in each specimen a method employing a weld embrittlement was developed. Using an Omark Gramweld stud welding machine at its lowest amperage output, a small 1/8 in. diameter stud was welded to the specimen. This introduced micro cracks into the specimen at the weld. The stud was then knocked off with a hammer and 45° angle saw cuts were introduced into the specimen from either side creating a sharp Vee in the area of desired crack initiation. Figure 5 shows the steps involved in this process.

Using the 10 ton Amsler Vibrophore, a high frequency fatigue testing machine, in a 3-point bend arrangement the crack was grown in two separate stages. For the first stage a large stress range was used to initiate the crack in a reasonable length of time. It was grown to approximately 1/2 in., within 200,000 cycles or 20 minutes.

The second stage, the final 1/4 in., was grown at a much smaller stress range to conform to the ASTM recommendation that the final rate of crack growth does not exceed 0.05 inch per 50,000 cycles.[1] The effect of this final slow growth stage was to reduce the size of the plastic zone preceding the crack and to force the crack to grow out of the larger zone of plastic disturbance produced in the first stage. It was found that the mean load need not be adjusted between the fast growth and slow growth because growth rate was controlled by load range rather than by mean load.

During the fatigue operations, plastic deformation occurred under the two reaction points and the load point. Pilot tests showed that an initial disturbance appeared in the load signal when the tup struck the indent in the top of the specimen caused during fatigue loading. Therefore the top surface of all specimens was machined to obtain a flat impact surface.

3. TEST APPARATUS

The testing machine, shown in Fig. 6, is a specially designed drop weight machine that can accommodate the testing of tear specimens from 1/2" to 2" in thickness. The main uprights are 12W85 sections with guide tracks along the inner face of either column that are adjustable for easy alignment.

The base anvil is a 6 in. thick steel block. The entire base weldment under the anvil is tied into a 4 ft. thick concrete slab with 3-1/2 in. diameter anchor bolts. The falling mass, a 200 lb. weight, can be dropped from any height up to 30 feet. Close tolerance of 1/16 inch between the weight and each guide track was held to ensure that the impact was on center minimizing random stress waves that could be set up due to eccentric loading of the specimen.

The impacting surface, as shown in Fig. 7, is a specially designed, removable, tup machined from 4340 steel heat-treated to Rc 50. The testing fixture that holds the specimen in position, Fig. 8, was also fabricated from heat treated steel and is bolted securely to the base anvil.

The 200 pound free falling weight is supported by an electro-magnetic release mechanism which is raised and lowered by a 2 ton overhead crane. To ensure maximum safety in the operation of the release mechanism two integrated electrical circuits are used. The

man who installs the specimen in the machine has to close one circuit before the actual weight release circuit is activated. The weight can then and only then be dropped by the operator at the control desk.

The cooling system, Figs. 9 and 10, consisted of two separate heavy oak boxes, one that enclosed the specimen on the base anvil and the other, which contained the cooling agent, located outside the safety gates. A fan located on the outer box circulated air over the cooling agent, through insulated copper tubing and around the specimen. The outer box was adaptable to either dry ice or liquid nitrogen as the cooling agent. Dry ice proved to be the most feasible and easiest to use.

Several alternates were tried to stop the falling weight after specimen fracture, the most successful being 2 in. thick laminated elastomeric bridge bearing pads mounted on 2 in. thick oak blocks. The blocks also acted as sides for the cooling box housing the specimen. Figure 10 illustrates their use and their condition after 70 to 100 tests.

4. INSTRUMENTATION

4.1 Introduction

Instrumentation was composed of three separate recording circuits. These circuits were used to monitor:

1. Load versus time during impact and fracture
2. Crack movement during fracture
3. Bending strains in the specimen during impact and fracture

4.2 Load-Time Record

The load-time record was obtained by instrumenting the tup with 1/4 in. electrical resistance foil strain gages. These gages were placed in a four arm bridge arrangement, one arm on each of the four sides of the tup as shown in Fig. 7. To obtain added output from this system 2 - 120 ohm gages were placed in series on each arm of the bridge, two arms in compression during impact and two in tension due to the Poisson effect.

This circuit gave an amplification factor of 2.6 to the output signal from the gages. Although the circuit would compensate for bending of the tup, eccentric loadings were generally undesirable and were minimized in the testing procedure. The bridge output was quite small because stresses in the tup were kept low (below 10,000 psi).

The output signal from the tup gages was transferred to the monitoring oscilloscope by copper shielded cable. Figure 11 shows the circuit diagram for the load signal. To reduce electrical noise all copper shields were grounded through the oscilloscope into the electrical wall socket. Even after the utmost precautions had been taken in the wiring system, sporadic signals could be picked up from the 20 ton overhead crane and from the strain gage digitizer being used on the laboratory floor. Testing had to be done when neither was in operation.

A Taktronix Type 549 storage oscilloscope with a type 1A1 dial trace vertical amplifier was used to monitor the output signal from the load circuit. The 1A1 amplifier has a maximum calibrated deflection of 5 mv/cm and a risetime of 16 ns. The vertical amplifier time response was an important consideration in oscilloscope selection as expected loading rates might be quite fast.

A multi-channel oscillograph was tried as an alternative to the oscilloscope but it was much too slow, even at its fastest writing speed.

In order to initiate the beam trace before impact, an external trigger source had to be used that would trigger the sweep of the oscilloscope at the proper moment. An internal trigger that started the sweep on the rising portion of the load curve could have been used, but this would have resulted in the loss of the initial portion of the load record. The system finally selected was a vacuum tube photocell powered by a DC power supply. This photocell was mounted in such a

manner that the falling weight would cut off the light beam so as to trigger the delay timing mechanism of the oscilloscope. After a preset time delay the electron beam would then sweep and temporarily store the load record on the oscilloscope screen.

The time delay was adjustable. It could be altered when different drop heights were used and also when specimen depth varied. Mathematical calculations using the basic equations of physics for free falling masses proved accurate enough for the proper delay setting. By setting the delay so that the actual load record started at mid-screen it was possible to see if there was any electrical noise or overriding signal on the beam trace. Such noise would have been evident on the initial portion of the sweep.

4.3 Crack Velocity Record

An attempt to measure crack velocity was made using Budd Type CP-1101EX crack propagation gages, Fig. 12, with an overall length of 1.92 inches and an overall width of 0.75 inch. Several gage positions were tried in order to determine exactly when the crack was moving with respect to the obtained record.

As the crack traversed upwards through the 20-wire gage, successive wire breaks provided incremental changes in gage resistance from 4 ohms with no wires broken, to 40 ohms with one wire remaining. These changes appeared as a step function on the oscilloscope trace. Due to the nonlinear characteristics of this step function an 1800 ohm resistor was placed in series with the gage. The result was to produce

a constant voltage change from each breaking wire. The circuit diagram is shown in Fig. 12.

4.4 Bending Strain-Time Record

In order to establish specimen response during the load cycle, a limited number of samples were gaged as shown in Fig. 13 to obtain a direct record of bending strain versus time. Since the oscilloscope had a dual trace vertical amplifier it was possible to monitor simultaneously the load record as indicated by the tup gages and the load record as indicated by the bending strains in the specimen.

The gages were set up in a full bridge arrangement 2-1/2 inches on either side of the crack and 1/2 inch from the upper and lower beam edges. It was felt that if the gages were placed at these locations the presence of the crack and the impacting tup would not influence the nominal strains which were recorded. Specimen calibration under static conditions and theoretical computation of bending strains agreed quite well. The gaged specimen and the electrical circuit are shown in Fig. 13.

4.5 Power Supply

All three monitoring systems needed a constant DC power source. Two 12 volt automobile batteries were used in series to drive the gages on the tup and one 12 volt battery was used to drive either the crack wire gage or the gages on the bend specimens. Only two of these circuits were used at the same time since the oscilloscope had the capability of monitoring simultaneously only two output signals.

Linear potentiometers across each power source allowed accurate setting of the voltage. Prior to testing voltage was checked with a digital voltmeter accurate to the nearest 1/10 of a volt. All shields from the power leads to the gages were grounded back through the scope to ensure a minimal amount of electrical noise on the trace.

4.6 Temperature Record

Temperature, an important variable in this series of tests, was constantly monitored. Electrical resistance temperature gages were mounted on the specimen surface near the root of the notch. To obtain the inner specimen temperature for a few of the tests an iron constantine thermocouple, covered with silicon gel for good heat conduction, was used. It was inserted in a 1/16 inch diameter hole on the upper edge of the specimen drilled to a depth of 3/4 inch. Temperature readings as indicated by the surface temperature gage and the thermocouple agreed to within 5 degrees Fahrenheit.

5. DESCRIPTION OF TESTS

5.1 Compliance Calibration

Gross and Srawley have derived a K calibration for the single edge-cracked plate specimen in three-point bending using a boundary collocation technique.[12] The limit of their analysis is for span to depth ratios (L/W) greater than 4. Below this ratio the accuracy of the K calibration is considered dubious because of the increasing difficulty of representing the physical loading conditions. Srawley's analysis is based on roller supports with no horizontal restraint.

The (L/W) ratio for the fracture specimens discussed in this report is 3.33, considerably less than the limit of Srawley's analysis. Furthermore the half-round supports of the testing fixture provide some horizontal restraint. To determine the effect of the increased depth and the rigid supports an experimental K calibration, developed by Irwin and Kies,[13] was carried out using an aluminum model with an (L/W) ratio of 3.33. Previous experimental compliance measurements have been done for specimens with (L/W) ratios of 8 and 10.[14,15]

The model, 24" x 6" x 1", was exactly twice the size of the steel prototype and fabricated from 7075-T6 high strength aluminum alloy. This model geometry and material gave a magnification in compliance of 1.41 over the prototype.

The specimen supports were the same as used for the fracture tests but extended to a span of 20 inches. Steel bearing pads and copper shims were used at the load point and the reaction points to prevent plastic indentation of the aluminum plate. The roller supports were covered with a thin layer of graphite lubricant to minimize frictional restraint.

Deflection was measured over the supports to detect permanent support settlement and at midspan to record the beam deflection. Ames dial gages accurate to ±.0001 in. were used.

The crack was extended in 1/4 inch increments with an ordinary band saw to a depth of 3-1/2 inches. After each increment the specimen was loaded as shown in Fig. 14 and the deflections were measured. Nominal stresses in the aluminum were kept below 0.6 σ_Y at all times. The first deflection measurement was always made under a preload of 2 kips.

Initially an effort was made to "shakedown" the specimen before measuring deflections by loading it to 0.6 σ_Y at least five times. Krafft recommends this procedure to eliminate any nonlinear portions of the load-deflection relationship and to strain-harden the region at the leading edge of the saw cut.[16] This "shakedown" procedure however had no effect on the load deflection relationship recorded in this test.

5.2 Preliminary Fracture Tests

In order to obtain a reliable and a meaningful load record it was necessary to carry out an extensive preliminary testing program.

The first tests utilized a pressed notch 0.16 in. deep. Interpretation of the records was unfortunately handicapped by large inertial effects and by the uncertain sharpness of the notch. To obtain data applicable to actual crack extension in bridge steels a deeper notch sharpened by fatigue cracking was necessary. Deepening the notch tended to shift the initation of crack extension to a time less influenced by the inertial loading impact.

Loading pads were tried in an effort to further reduce the impact (inertial) effect. These consisted of two different diameter brass bars 3/32 in. and 9/32 in. and half round slugs of copper, brass, steel, or aluminum. Another approach utilized a 11/32 in. thick rubber washer inserted between the removable tup and the weight. It was felt that if the loading time to fracture could be spread out to approximately 0.5 milliseconds a quasi-static analysis could be applied to the dynamic records. Final cushion selection was a 1/2 in. diameter half round pad of 2024 aluminum oriented on the specimen as shown in Fig. 15. Using this cushion the tup load record showed a gradual rise to the point of onset of rapid cracking over a time of 0.4 to 0.8 milliseconds.

It was found that the impact or inertia effect could be minimized on unpadded specimens by lowering the drop height to a point where there was just sufficient energy to cause fracture. Tests on the 1/2 in. plate which were initially from a drop height of 10 feet were later lowered to a drop height of 1 foot or less. At warmer temperatures a greater drop height was needed to cause fracture. When the point was reached

where a 2 foot drop did not cause fracture, a loading cushion had to be used since inertial effects would completely override the load signal.

5.3 Test Procedure

After the preliminary fracture tests the following conditions for testing were set up:

1. Conduct tests from a minimum drop height needed to cause fracture.
2. Conduct one set of tests with no loading cushion.
3. Conduct one set of tests with a half round aluminum pad as a loading cushion.

Thereafter, the testing procedure was the same for all specimens except for the variation of temperature, loading cushion, and drop height. A temperature gage on an aluminum strip was mounted on the surface of the specimen close to the notch with electrical tape. Both reaction points on the fixture and the tup were covered with a fine coating of a graphite lubricant in an effort to provide friction free contact. The specimen was inserted into the 3-point bend fixture and aligned to insure impact directly over the fatigue crack. After alignment the cooling box was closed and saran wrap was taped across the hole in the top of the box through which the falling tup would pass.

The length of cooling time depended on desired test temperature, being approximately 45 minutes for a -40° F test. The specimen remained at its test temperature for at least 20 minutes to insure an even temperature distribution through the plate thickness. Prior to the

actual drop, voltages across the load circuit and either the crack wire or the bend specimen circuit were checked with a digital voltmeter and adjusted to exactly 22 volts and 12 volts respectively by using the potentiometer in each circuit.

At the beginning of each day of tests the oscilloscope was calibrated using its built-in resistance and adjusted if necessary. As a final check on the triggering system an opaque sheet was passed in front of the photocell to activate the sweep. The saran wrap covering the opening in the top of the specimen cooling box was removed a moment before the weight was dropped.

After the drop a Polaroid photograph was taken of the trace that had been stored on the oscilloscope screen. The specimen was removed from the fixture and the fracture surface sprayed with CRC-3-36 surface coating to prevent rusting.

5.4 Test Schedule

Table 2 shows the testing schedule that was followed. The tests were carried out at four test temperatures: -90° F, -40° F, 0° F, and $+30^{\circ}$ F. Those at -90° F were conducted by packing the specimen in dry ice for several hours and then transferring to the test fixture on the base anvil. A valid test for an unpadded specimen could not be obtained at $+30^{\circ}$ F. At this temperature the drop height needed to initiate fracture was greater than 2 feet thereby causing the inertia effect from the striking impact to override the load record.

6. THEORETICAL ANALYSIS

6.1 Linear Crack Stress Field Analysis

Using a Westergaard type linear elastic stress solution, Irwin obtained the stresses close to the leading edge of a crack.[17] For a Mode I (opening tensile mode) type of fracture he represented these stresses as follows:

$$\sigma_y = \frac{K_I}{\sqrt{2\pi r}} \cos\frac{\theta}{2}\left[1 + \sin\frac{\theta}{2}\sin\frac{3\theta}{2}\right] \qquad (6.1a)$$

$$\sigma_x = \frac{K_I}{\sqrt{2\pi r}} \cos\frac{\theta}{2}\left[1 - \sin\frac{\theta}{2}\sin\frac{3\theta}{2}\right] \qquad (6.1b)$$

$$\tau_{xy} = \frac{K_I}{\sqrt{2\pi r}} \sin\frac{\theta}{2}\cos\frac{\theta}{2}\cos\frac{3\theta}{2} \qquad (6.1c)$$

$$\sigma_z = \mu\,(\sigma_x + \sigma_y) \quad \text{(plane strain)} \qquad (6.1d)$$

or

$$\sigma_z = 0 \quad \text{(plane stress)} \qquad (6.1e)$$

where the coordinates are as shown in Fig. 16.

The stress intensity factor, K_I, is a parameter which characterizes the stresses tending to cause crack extension. It is proportional to applied stress and a function of the crack length,

specimen size, and specimen geometry. If the crack tip plastic zone is small enough for essentially plane strain conditions during the abrupt development of rapid crack extension, then the K factor is termed K_{IC} at the point of crack instability.

Two types of fracture conditions are possible at the leading edge of the crack: plane stress or plane strain. For a through crack in a thin plate a plane stress situation is present due to lack of elastic constraint through the thickness ($\sigma_z = 0$). Even if the plastic zone is relatively small compared to the plate thickness, a plane stress condition exists on the outer edges. In this case the stresses found from Eqs. 6.1a, 6.1b, and 6.1c are taken as averages through the plate thickness.

Irwin has introduced a plastic zone correction that must be added to the original crack length "a_o" to correct this solution for the zone of plastic yielding at the leading edge of the crack.[18] For a plane stress solution this correction is:

$$r_Y = \frac{1}{2\pi} \left(\frac{K}{\sigma_Y}\right)^2 \qquad (6.2)$$

where

$2r_Y$ = plastic zone size as shown in Fig. 16

K = stress intensity factor

σ_Y = yield strength of material

6.2 Brittle-Ductile Fracture Transition

As previously mentioned there is always a small amount of plane stress area present on the outer edges of the plate under tensile loading. This fact is exemplified by the shear lips present on a fracture surface. As a condition of 100% plane strain is approached, the size of these lips decreases and a pure Mode 1 type of fracture is approached.

Fracture investigations of the Polaris and Minuteman programs indicated that the percentage of oblique shear on the fracture surface was related to the dimensionless ratio β_c where:[19]

$$\beta_c = \frac{1}{B}\left(\frac{K_C}{\sigma_Y}\right)^2 \qquad \text{(plane stress)} \qquad (6.3)$$

References 20 and 21 noted that less than 50% shear was usually present when $\beta_c < \pi$. This observation of a brittle ductile transition at $\beta_c = \pi$ leads to a plastic zone size in the range of the plate thickness.

To correct for the influence of plastic flow indicated by the oblique shear portion of the fracture surface, the following equation can be used if $\beta_c < \pi$.[22]

$$K_{IC}^2 = \frac{K_C^2}{1 + 0.5\,\beta_c} \qquad (6.4)$$

where

K_{IC} = plane strain fracture toughness for a Mode 1 failure

K_C = stress intensity factor at onset of rapid fracture

6.3 Experimental Analysis

The experimental determination of K and K_C, in particular, can be accomplished using a compliance technique. A load-deformation curve is shown in Fig. 17 for a bend specimen with an initial edge crack length "a_o" and after an incremental crack growth of "da". The compliance of the specimen is a function of applied load and crack length.

$$y = C\,P \tag{6.5}$$

where

y = amount of specimen deflection

C = specimen compliance

P = applied load

The shaded portion indicates the amount of strain energy, dU, lost due to crack extension. It is this energy loss that Griffith assumed must exceed the gain in surface energy for rapid crack extension to occur.[7] Knowing that this loss of energy equals "$\mathcal{G}\,da$", it can be shown that

$$\mathcal{G} = \frac{1}{B}\frac{P^2}{2}\left(\frac{dC}{da}\right) \tag{6.6}$$

where

$\mathcal{G}$ = energy loss per unit of plate thickness B due to a small increment of crack extension, "da".

dC/da = rate of change of specimen compliance with crack length

B = plate thickness

P = applied load

For tensile cracks $\mathcal{G}$ can be related to K^2 by the following formulae.

$$\mathcal{G} = \frac{K^2}{E} \qquad \text{for plane stress} \qquad (6.7a)$$

$$\mathcal{G} = (\frac{K^2}{E})(1 - \mu^2) \qquad \text{for plane strain} \qquad (6.7b)$$

where

E = modulus of elasticity of material

μ = Poisson's ratio

In this work the plane stress analysis was appropriate regardless of the local stress state at the leading edge of the crack. Rearranging terms, the expression for K^2 takes the form

$$K^2 = \frac{1}{2W} \frac{P^2}{B^2} \frac{d(ECB)}{d(a/W)} \qquad (6.8)$$

For a three-point bend specimen Gross and Srawley have developed the following K_I calibration using a boundary collocation technique.[12]

$$Y = \frac{K_I \, BW^2}{6 \, Ma^{1/2}} = A_o + A_1(a/W) + A_2(a/W)^2 + A_3(a/W)^3 + A_4(a/W)^4 \qquad (6.9)$$

where

Y = dimensionless ratio

W = specimen depth

M = 1.5 PL = applied bending moment

P = applied load

L = span length

A = coefficients depending on span length to beam depth ratio

and

$$a = a_o + r_Y$$

where

$_{o}$ = original crack length

r_Y = plastic zone correction (see Eq. 6.2)

The Gross and Srawley solution is limited to a minimum span length to beam depth ratio (L/W) of 4. Below this value the boundary collocation solution loses accuracy because it does not adequately represent the physical loading conditions.

Since the (L/W) ratio for the specimen of this series of tests is 3.33 it was decided to carry out a compliance calibration on an aluminum model.

6.4 Dynamic Yield Strength

The experimental investigation of this report is concerned with rapid strain rates and various specimen temperatures. The combination of these two variables affect the yield strength of the material considerably, that is, a high strain rate and a low temperature both cause an increase in the yield strength.

A recent paper by Wessel et al. provides measurements of yield strength of A302B steel for various temperatures from -320° F to room temperature.[23] A good fit to this data was obtained by the expression[24]

$$\sigma_Y \Big|_{T,t_o} = \sigma_Y \Big|_{+75^o\ F,t_o} + \frac{14,500}{T + 459} - 27.4 \qquad (6.10)$$

where

T = specimen temperature in ^oF

t_o = load rise time for static test (50 sec.)

If the loading time is shorter than t_o, the temperature-rate equivalence idea leads to the relations

$$\sigma_Y \Big|_{T,t} = \sigma_Y \Big|_{T',t_o}$$

where

$$\frac{T' + 459}{T + 459} = \frac{\log(2 \times 10^{10}\ t)}{\log(2 \times 10^{10}\ t_o)} \qquad (6.11)$$

Combination of the two expressions, 6.10 and 6.11, leads to the following equation which accounts for the affect of both temperature change and strain rate on yield strength.

$$\sigma_Y \Big|_{T,t} = \sigma_Y \Big|_{+75^o\ F,t_o} + \frac{174{,}000}{\log(2 \times 10^{10}\ t)(T + 459)} - 27.4$$

(6.12)

7. ANALYSIS AND DISCUSSION OF TEST RESULTS

7.1 Compliance Calibration

The procedure used for the reduction of the experimental data was to use Gross and Srawley's curve of Fig. 18 with Y versus (a/W) for an (L/W) ratio of 3.33 and integrate to find the proper compliance versus (a/W) relationship.

The derived compliance function was of the polynomial form

$$C = C_o + C_1(a/W) + C_2(a/W)^2 + C_3(a/W)^3 + C_4(a/w)^4 + C_5(a/W)^5 \qquad (7.1)$$

Boundary conditions dictated the value of the terms C_1 and C_2. Because $K = f(\frac{dC}{d(a/W)})$, the term C_1 was forced to zero. The value of C_2 was determined from the condition that as (a/W) approaches zero the value of Y, as defined in Eq. 6.9, approaches 1.93. This is equivalent to saying K approaches that of a free edge condition.

The final compliance equation as determined from the boundary collocation solution of Gross and Srawley was as follows:

$$C = [8.472 + 63.75(a/W)^2 - 124.6(a/W)^3 + 373.7(a/W)^4 - 254(a/W)^5] \times 10^{-4} \qquad (7.2)$$

Comparison of Eq. 7.2 to the data points of the compliance calibration is shown in Fig. 19. For a/W ratios less than 0.1 the derived function does not follow the data because of the second imposed boundary condition. In the (a/W) region of practical importance, that is, between 0.1 and 0.40 the agreement is quite acceptable.

Since the boundary collocation solution was found to be applicable to our specimen geometry it was used for all data reduction.

$$\frac{K_I\, BW^2}{6M\sqrt{a}} = 1.93 - 3.12(a/W) + 14.68(a/W)^2 - 25.3(a/W)^3 + 25.90(a/W)^4 \qquad (7.3)$$

7.2 Load-Time Records

7.2.1 Pressed Notch versus Fatigue Crack - Preliminary tests were performed on specimens with a pressed notch 0.16 in. deep in the hope that valid K_C results could be obtained. Thereby it would be possible to correlate the industrial drop weight tear temperature transition approach with the fracture toughness parameter K_C. Figure 20 shows the load-time curve of both a pressed notch and a fatigue cracked specimen for a 4 foot drop.

The main comparison to be made here is the general pattern of the two curves. The specimen with a pressed notch indicates a peak load being reached but being held for a finite amount of time, approximately 0.2 ms, before actual fracture occurs, and even then, fracture occurs only after application of a reflected shock wave indicated by the second

peak on the record. The specimen with the fatigue crack shows a rising load to a peak where fracture occurs abruptly.

Comparison of the two results and confirmation by a crack wire record indicates that the crack in the pressed notch specimen did not start to move upon leveling off of the load. It appears as though the pressed notch does not simulate the behavior of an actual sharp crack. On this premise, and on the fact that the ASTM committee E24 recommends the use of fatigue precracked specimens for K_{IC} determination, a fatigue crack was considered mandatory for valid test results.[1] Of the few tests that were run on pressed notch specimens it was found that the fracture load was not consistent. It varied with drop height, the higher height giving a higher fracture load.

As will be shown later, even the lower record in Fig. 20 will not give a valid result because of inertial effects.

7.2.2 Influence of Drop Height - Figure 21 shows how reduction of drop height affects the load record for an unpadded specimen. A four foot drop results in a single impact spike that completely obliterates the load that the specimen feels. As the drop height is decreased a double peaked record forms with the first spike being due to inertia affects alone and the second being more nearly the true load that the specimen feels at fracture. The third record with a 1 foot drop confirms the fact that the impact peak is a function of drop height whereas the fracture load remains unchanged.

Explanation of the decreasing magnitude of the inertia spike is quite simple. As the drop height is decreased the velocity of the

weight at point of impact also decreases. This causes the specimen to accelerate at a slower rate and thereby to exert a lower inertia force on the tup.

The fact that most of the specimen does not respond to this initial inertia spike was validated when strain gages on the specimen and the load from the tup were monitored simultaneously. The gages on the specimen indicated a smooth rising load to fracture whereas the tup load record was double peaked in nature.

7.2.3 Padded versus Unpadded Specimen - It was stated that the 4 foot drop on the unpadded specimen in Fig. 20 would not give a valid test result. Figure 22 shows a comparison between a padded and an unpadded specimen for the same drop height, 4 feet. The aluminum pad spreads out the load to approximately 0.8 ms and indicates a peak load of 8.0 kips. The unpadded specimen shows a maximum load of 20.0 kips. It is quite obvious from this latter result that the inertia effects of the unpadded specimen completely obscured the actual load record. For this reason the test of an unpadded specimen was considered useful only when the load record was double peaked in nature.

7.2.4 K_C and K_{IC} Computation - Figure 23 illustrates both a double peaked record and a padded record from which useful K_C values were obtained. For K_C computation the peak load in either case was assumed to be the fracture load. Measurements of this peak load (P) and the time from load initiation to fracture (t) were made from the Polaroid photographs of the oscilloscope traces. The length of the precrack, a_o, was measured after the test using a weighted averaging

procedure of 3 crack length measurements. The length at midthickness was weighted with a factor of 2 whereas the crack lengths at 1/4 thickness were weighted with a factor of 1. This procedure provides a suitable averaging method for the normal crescent shape of the leading edge of the crack.

By the use of an iterative procedure, K_C was calculated for each specimen using Eqs. 6.2 and 7.3 with the specimen and crack size factors B, W, and a_o.

Sample hand calculations of K_C and K_{IC} can be found in Appendix A. Confidence of the validity of this dynamic approach to measure fracture toughness was assured by the comparable K_C and K_{IC} results obtained from both padded and unpadded tests.

A computer program was used for K_C and K_{IC} computations. The program started by assuming a plastic zone size $(r_Y)_1$ of zero, calculating K_C and then recalculating another plastic zone size $(r_Y)_2$. This iteration was continued until convergence of zone size occurred to the desired accuracy. A flow chart for this program is shown in Fig. 24.

The yield strength σ_Y used in these calculations was elevated due to high strain rate and low temperature. Therefore σ_Y (dynamic) had to be initially computed from Eq. 6.12. With a known K_C, the plane strain fracture toughness K_{IC} was found from Eq. 6.4 which corrected approximately for plane stress areas on the fracture surface.

The use of Eq. 6.4 is governed by the factor β_c being less than π. This condition limits the area of oblique shear on the fracture surface to less than 50% and clearly represents a midrange condition

for the transition from a flat tensile fracture to one of increased fracture toughness. Therefore the limiting value of K_C that can be corrected for plane stress area is determined as follows.

$$\beta_c < \frac{1}{B} \left(\frac{K_C}{\sigma_Y}\right)^2$$

$$\therefore K_C^2 < \pi \times (\sigma_Y)^2 \times B$$

where

$$\sigma_Y = 85 \text{ ksi (assumed)}$$

$$\therefore K_C < 107 \text{ ksi } \sqrt{\text{in.}}$$

Figure 25 plots K_C against test temperature for all specimens. There is no demarcation made between longitudinal and transverse specimens or padded and unpadded because no significant trend was found in either case. The curve is a least squares fit to a power series of third degree. All the test points can be corrected for plane stress areas using Eq. 6.4. At $+40^{\circ}$ F, $\beta_c \simeq \pi$ which indicates this to be the brittle-ductile transition point.

The corrected curve of K_{IC} versus temperature is shown in Fig. 26 with a band of ±5 ksi $\sqrt{\text{in.}}$ showing the limits of experimental confidence. This confidence band was determined from the accuracy with which measurements could be made of the fracture load and the precracked length. The plot is linear in nature and most test points lie within the confidence zone.

Figure 27 shows how the K_C and K_{IC} curves relate to each other. Note that the correction for plane stress increases substantially with increasing temperature.

7.3 Crack Wire Records

Crack wire records and load records were obtained simultaneously during a test using the dual trace amplifier of the oscilloscope in the "chop" mode. Figure 28(a) is a typical record of such a test on an unpadded specimen with a fatigue crack. The gage was placed so that the first wire was at the leading edge of the fatigue crack and the drop height was one foot, which was low enough to cause a double peaked record.

The crack wire record is a discontinuous step curve set up by the successive breaking of each individual gage wire spaced at intervals of 2.5 mm. If one can assume that the wires are not breaking due to bending of the specimen before the crack reaches them or due to movement of the plastic zone preceding the moving crack, then this record should be a true picture of the crack movement on the plate surface as a function of time.

The validity of these assumptions is difficult to substantiate as only high speed photography could show actual gage response with respect to the moving crack. The first assumption can be rationalized by the fact that very little bending takes place before a brittle fracture occurs, probably an amount insufficient to cause the wires to break. The second assumption is not quite as easy to substantiate. Since the gage is completely bonded to the specimen it would seem possible that the zone of plastification which precedes the crack could cause wires to break before the crack actually reaches them. If this

were the case, the record would indicate the velocity of the moving plastic zone rather than that of the crack.

An interesting observation was made after each crack wire test. The gage did not fail by severing down the middle into two pieces as would be expected but rather by severing down either side of the crack, leaving a long thin strip of gage about 1/16 in. wide in one piece. It would appear as though this strip could be indicative of the size of the moving plastic zone, which is in reality a "butterfly" shape. If such is the case the zone size seems to remain constant once the crack starts to move.

Reference again to Fig. 28(a) shows that there is a finite amount of time before the crack reaches a uniform running speed, approximately 0.17 ms. After this acceleration interval the crack speed is constant at 1025 ft/sec for the major portion of the fracturing process. When the crack reaches a point approximately 1/2 inch from the upper surface of the specimen it arrests and final separation does not take place until the specimen feels another load impulse caused by the elastic shock wave returning from the 200 lb. weight. The natural period of this shock wave is approximately 0.20 ms and can be followed throughout the record from the time of peak load to the time of complete fracture.

Figure 28(b) is a crack wire record for a specimen containing a pressed notch tested at 0° F. Since this gage was placed so that the middle of the gage was at the mid-depth of the specimen, no acceleration period is noted. The crack had moved 3/8 in. before it broke the

first wire. The point to note is that the maximum surface crack speed for this test was 2100 ft/sec. which was much faster than was found for the fatigue cracked specimen.

According to the theoretical fracture mechanics and a study by Yoffe the limit to the speed of a crack fixed by inertia is the Rayleigh wave velocity.[25] For a purely brittle crack this limit is 0.9 C_2 where C_2 is the elastic shear wave velocity. The highest velocities yet observed have been 0.6 C_2 in pure silica glass. In steels, crack velocities are usually below 5000 ft/sec. The elastic shear wave velocity C_2 is 10,450 ft/sec. for steel; therefore the maximum observed crack speed as indicated by the crack wire record is about 0.2 C_2. Comparison of the K_C value for the two crack wire records show that the pressed notch is higher by 6 ksi $\sqrt{in}$. Since crack speed increases with the driving force it would be expected that the crack in the pressed notch specimen would move faster.

Reference again to Fig. 28(a) indicates that the crack wire gage senses the moving crack before the tup does. As will be seen later this fact is also verified by the bend specimens. The reason for this delay is due to the tensile unloading waves set up by the moving crack. The tup will not feel a drop in load until these waves are reflected back to the point of impact. The magnitude of this delay can be approximated as 1/2 natural period of specimen plus 0.1 ms, where the latter term is the time taken for the elastic shear wave to travel 12 inches (that is, from the crack to the support reaction and back to the

tup). The natural period of the 1/2 inch plate specimen is 0.300 ms leading to a delay time of 0.25 ms. Correspondingly, the record indicates a delay of 0.23 ms.

7.4 Bending Strain - Time Records

Again using the dual trace features of the oscilloscope a limited number of specimens were tested monitoring simultaneously bending strains in the specimen and the load record indicated by the tup. The result of such a test is shown in Fig. 29, the upper trace being the load and the lower trace being the bending strains. The specimen was padded and the drop height was 4 feet.

As with the crack wire record, the bending gages indicate that the crack is moving before the tup senses a peak load. The time delay between the two records is 0.28 ms which again is close to the approximated value of 0.25 ms.

Although both traces reach a peak at a different time the maximum load recorded by each is close and leads to comparable K_C values, 49.6 ksi $\sqrt{in.}$ for the tup record and 53.2 ksi $\sqrt{in.}$ for the beam record. This discrepancy is well within the confidence limits of measuring ability.

By the use of the aluminum loading pad, the load has been spread out to 0.28 ms, as indicated by the bending gages, a value quite close to the natural period of the specimen, 0.30 ms. It appears as though this is sufficient for a quasi-static stress state to be set up as

both the tup and the specimen then indicate the same load at the fracture point.

Appendix B contains a simple dynamic analysis of the system using the load record of Fig. 29 as a forcing function and comparing the result with the bending record of the lower trace.

7.5 ASTM Specimen Geometry Recommendations

The accuracy with which K_{IC} describes the fracture behavior of a material depends on the condition of stress and strain at the leading edge of the crack. Theoretically K_{IC} gives an exact tepresentation only in the limit of zero plastic strain. Therefore to obtain a satisfactory approximation of the fracture toughness the relative size of the plastic zone at the crack tip must be limited.

For static testing, ASTM Committee E24 has recommended the following specimen size requirements:[1]

$$\text{Specimen thickness} \qquad B \geq 2.5 \left(\frac{K_{IC}}{\sigma_Y}\right)^2 = 2.5\ \pi(2\ r_Y)$$

$$\text{Crack length} \qquad a_o \geq 2.5 \left(\frac{K_{IC}}{\sigma_Y}\right)^2$$

$$\text{Ligament length} \qquad \frac{W - a_o}{W} \geq 2.5 \left(\frac{K_{IC}}{\sigma_Y}\right)^2$$

For the dynamic tests of this report it was assumed that all K values were K_C values, not K_{IC}, and thereby had to be corrected for plane stress areas using Eq. 6.4.

Comparison to these limitations provides an idea of what temperature is low enough such that the reported tests are actually yielding K_{IC} values rather than K_C.

Using the thickness limitation:

$$B \geq 2.5 \left(\frac{K_{IC}}{\sigma_Y}\right)^2$$

where

$B = 0.5$ in.

$\sigma_Y = 90$ ksi (average)

$\therefore K_{IC} \leq 40$ ksi $\sqrt{\text{in.}}$

The data of Fig. 26 show that approximately -100° F is the maximum testing temperature for a valid K_{IC} test. Thus the K_C, K_{IC} curves of Fig. 27 should be coincident at temperatures below -100° F.

Using the crack length limitation yields

$$K_{IC} < 49 \text{ ksi } \sqrt{\text{in.}}$$

thus the thickness requirement governs.

7.6 Comparison Between Dynamic Fracture Toughness Measurements and Fracture Transition Temperature Measurements

The results of an NDT drop weight test, a transition temperature approach, can be correlated to dynamic fracture toughness measurements by the use of a fracture model. At the NDT temperature the stress level for crack propagation is close to the dynamic yield strength of the material.

Irwin and Puzak at the Naval Research Laboratory have taken a typical fractured NDT specimen as shown in Fig. 30 and made some estimates as to the initial crack dimensions at the point of the brittle weld bead.[26]

The K factor for a semi-elliptical surface flaw is

$$K^2 = \frac{1.2\ \pi\ \sigma^2}{\Phi^2 - 0.212(\frac{\sigma}{\sigma_Y})^2}$$

where

Φ = elliptical integral

$\sigma = \sigma_Y$ (dynamic)

For the crack shown in Fig. 30 this formula reduces to

$$K_{IC} = 0.78\ \sqrt{in.}\ \sigma_Y$$

K_{IC} is the dynamic fracture toughness of the material at the NDT and can be designated by K_{Id}.

For the 1/2 inch plate the NDT is approximated by the FATT, from the industrial drop weight tear test, minus 60^o F. This leads to an approximate NDT of $+20^o$ F. Assuming a loading time of 0.5 ms for an NDT test, a temperature of $+20^o$ F and a static yield strength of 56.9 kis results in a dynamic yield strength of 81 ksi using Eq. 6.12. The dynamic fracture toughness prediction becomes

$$K_{Id} = 0.78 \times 81 = 63.2\ \text{ksi}\ \sqrt{in.}$$

The actual K_{IC} (dynamic) estimated at $+20^{o}$ F from the data of this project was 58.3 ksi $\sqrt{in}$. The moderate difference of the two estimates is not significant in view of the approximate nature of the estimation procedure.

7.7 Fracture Surfaces

The fracture surfaces of pressed notch and fatigue cracked specimens are shown in Fig. 31(a) and (b).

The testing temperatures for the pressed notch specimens range from $+120^{o}$ F to 0^{o} F with the amount of shear lip present on the fracture surface increasing with temperature to a near 100%. The small amount of plane strain area at the root of the notch for the $+120^{o}$ F specimen is due to the triaxiality of stresses set up by the pressing operation. These four specimens were part of the series used to determine the 50% FATT of 80^{o} F as shown in Fig. 2.

Figure 31(b) is a series of fracture surfaces of fatigue cracked specimens ranging in temperature from $+30^{o}$ F to -90^{o} F. The lighter and darker layers on the fatigue surfaces indicate the different stress ranges used to grow the crack with a high range for crack initiation and a much smaller range for the final 1/4 inch of growth.

As with the pressed notch specimens the amount of shear lip increases with test temperature thereby raising the K_{C} values in a non-linear manner. Surface roughness also increases with temperature which is indicative of the branching characteristics of faster moving cracks. The higher K_{C} initiation values provide a greater driving force and thereby a higher crack velocity.

Comparison of Fig. 31(a) and (b) indicate that the crack velocity in a pressed notch specimen is much greater than a fatigue cracked specimen tested at the same temperature. This fact would tend to indicate that the pressed notch is not as severe as a fatigue crack and thereby would yield higher K_C values.

8. SUMMARY AND CONCLUSIONS

The results of this study indicate that the drop weight tear test can be used for the measurement of dynamic K_C if the proper testing procedure is adopted.

1. The specimen must contain a starting crack introduced by fatigue. The final amount of fatigue crack growth should conform to the ASTM recommendation of growth rate not to exceed 0.05 in. per 50,000 cycles.

2. Tests can be conducted on either padded or unpadded specimens. The pad found to be most satisfactory was a 1/2 inch diameter, half round cushion of 2024 aluminum which spread out the loading time to a time greater than the natural period of the specimen.

3. To minimize the inertial forces of an unpadded test the drop height must be low enough so that a double peaked record is obtained. The first peak is due to inertial effects and the second peak is the actual load felt by the specimen.

4. A quasi-static analysis can be used on either a padded or unpadded test provided the conditions above are satisfied. The assumption is made that fracture occurs when the load reaches a peak value. (Second peak on an unpadded record.)

5. The K_{IC} value obtained from the drop weight tear test agrees within 10% with the crack toughness estimated from the ductile-brittle transition temperature by Irwin's method, Ref. 24.

Additional tests conducted in the study indicate that:

1. The surface crack speed for a fatigue cracked specimen at -34^{o} F is approximately 1000 ft/sec. as indicated by crack wire gages.

2. The roughness of the fracture surfaces is indicative of the crack speed. The rougher surface of the faster moving crack shows its branching characteristics.

3. The load recorded by the tup and the bending strains recorded by the specimen are out of phase by about 1/4 ms as expected from dynamic considerations. Both records indicate the same peak load at fracture.

4. The compliance calibration indicates that the extrapolated K calibration based on Gross and Srawley's boundary collocation analysis is applicable to an (L/W) ratio of 3.33. The restrained roller supports do not seem to affect this calibration.

9. ACKNOWLEDGMENTS

This report presents partial results of the project entitled "Fracture Behavior of High Strength Low Alloy Structural Steels for Bridges" conducted at Fritz Engineering Laboratory of Lehigh University, Bethlehem, Pennsylvania. Dr. D. A. VanHorn is Chairman of the Department of Civil Engineering and Dr. L. S. Beedle is Director of the Laboratory. The project is under the directorship of Dr. G. R. Irwin, Boeing Professor at Lehigh University. The material tested throughout this investigation was supplied through the courtesy of the Bethlehem Steel Corporation, the sponsor of the project.

The authors wish to thank Mr. Marshall E. Pryor of Tektronix Inc., Mr. Hugh Sutherland of Fritz Engineering Laboratory and numerous persons at Homer Research Laboratory for their aid and assistance in developing the instrumentation used for this investigation.

Special thanks are due Dr. Roger G. Slutter for reviewing the manuscript, Mrs. Dorothy F. Fielding who typed and aided in its preparation, Mr. Richard Sopko for his photographic work, and Mrs. Sharon Balogh who prepared the drawings.

10. NOMENCLATURE

a	effective crack length, in.
a_o	initial crack length, in.
A_0, A_1, A_2	coefficients determined from compliance calibration
B	plate thickness, in.
C	compliance, in./lb.
dC/da	change in compliance with unit crack extension, $lb.^{-1}$
C_2	elastic shear wave velocity, ft./sec.
cm	centimeter
da	increment of crack extension
DWT	drop weight test
DWTT	drop weight tear test
E	uniaxial tensile (Young's) modulus, psi
FATT	fracture appearance transition temperature
$\mathcal{G}$	strain energy release rate, $in\text{-}lb./in.^2$
K	stress intensity factor, ksi $\sqrt{in.}$
K_C	critical stress intensity factor, ksi $\sqrt{in.}$
K_I	stress intensity factor for opening mode of crack surface displacement (tensile), ksi $\sqrt{in.}$
K_{IC}	critical stress intensity factor for opening mode of crack surface displacement, ksi $\sqrt{in.}$
L	span length, in.
M	specimen mass, $lb\text{-}sec^2/in.$
mm	millimeter

NOMENCLATURE (continued)

ms	millisecond
mv	millivolt
NDT	nil ductility transition temperature
NP	natural period of specimen, sec.
ns	nanosecond, (10^{-9})
P	applied load, lb.
r	radial position coordinate measured from leading edge of the crack, in.
r_Y	plasticity adjustment factor, in.
S	specimen stiffness, lb/in.
t	loading time to point of fracture, sec.
T	temperature, ^oF
W	specimen depth, in.
Y	dimensionless ratio relating stress intensity factor to crack length
y	specimen deflection in dynamic analysis, in.
$\ddot{y}$	specimen acceleration in dynamic analysis, $in/sec.^2$
β_c	dimensionless ratio relating plastic zone size to plate thickness
θ	angular position coordinate measured from the apparent leading edge of the crack
μ	Poisson's ratio
σ_Y	yield strength of material, ksi
σ_x	tensile stress component parallel to the plane of a crack in the X coordinate direction, ksi

NOMENCLATURE (continued)

σ_y	tensile stress component normal to the plane of a crack in the Y coordinate direction, ksi
σ_z	tensile stress component parallel to the leading edge of the crack in the Z coordinate direction, ksi
τ_{xy}	shearing stress in Y direction on a plane perpendicular to X, ksi
Φ	elliptic integral function

APPENDIXES

APPENDIX A

Sample Calculation of K_C and K_{IC}

The padded specimen of Fig. 23 will be used for the sample calculation.

Test Data

Test Temperature	-40°	F	(T)
Specimen Depth	2.92	inches	(W)
Weighted Crack Length	0.980	inches	(a_o)
Fracture Load	8.0	kips	(P)
Loading Time	0.55	ms	(t)
Static Yield Strength	56.9	ksi	

K_C Calculation

From Eq. 6.12

$$\sigma_Y = 56.9 + \frac{174{,}000}{\log(2 \times 10^{10} \times .55 \times 10^{-3})(-40 + 459)} - 27.4$$

$$\sigma_Y = 88.5 \text{ ksi}$$

Trial No. 1

Assume $r_Y = 0$

$$\therefore a = a_o + r_Y = 0.980 \text{ inches}$$

from Eq. 6.9

$$\frac{K_C\ BW^2}{6M\ a^{1/2}} = 1.93 - 3.14\left(\frac{0.98}{2.92}\right) + 14.68\left(\frac{0.98}{2.92}\right)^2 - 25.3\left(\frac{0.98}{2.92}\right)^3 + 25.9\left(\frac{0.98}{2.92}\right)^4 = +1.892$$

$$K_C = \frac{(1.892)(6)(8.0)(10.0)\sqrt{.980}}{(4)(0.5)(2.92)^2}$$

$$K_C = 53.21 \text{ ksi } \sqrt{\text{in.}}$$

K_{IC} Calculation

From Eq. 6.3 and 6.4

$$K_{IC} = \left[\frac{(53.21)^2}{1 + 0.5\left(\frac{53.21}{88.5}\right)^2\left(\frac{1}{0.5}\right)}\right]^{1/2}$$

$$K_{IC} = 45.60 \text{ ksi } \sqrt{\text{in.}}$$

r_Y Calculation

From Eq. 6.2

$$r_Y = \frac{1}{2\pi}\left(\frac{53.21}{88.5}\right)^2$$

$$r_Y = 0.0575 \text{ inches}$$

Trial No. 2

Assume $r_Y = 0.0575$ inches

$\therefore a = 0.980 + 0.0575 = 1.0375$ in.

Repeating the process of Trial No. 1 until the assumed and the calculated values of r_Y are within a difference of 0.0005 inches, the final results are:

K_C = 56.37 ksi $\sqrt{in.}$

K_{IC} = 47.54 ksi $\sqrt{in.}$

r_Y = 0.0645 inches

APPENDIX B

Dynamic Analysis

Using the record obtained in Fig. 29, a dynamic analysis of the problem was attempted utilizing the theory of simple structural dynamics.[27]

A. Stiffness of Specimen:

The stiffness of the specimen was determined from the compliance curve of Fig. 19, which takes into account the presence of the crack. For an a/W of 0.291 the compliance is 12.93×10^{-4} in./kip. Since stiffness (S) equals the inverse of the compliance

$$S = \frac{1}{12.93 \times 10^{-4}}$$

$$= 774 \text{ kip/in.}$$

B. Numerical Analysis

The load was approximated by three straight lines as shown below. It was considered to be acting as a forcing function P(t) on a specimen with a stiffness of 774 kip/in.

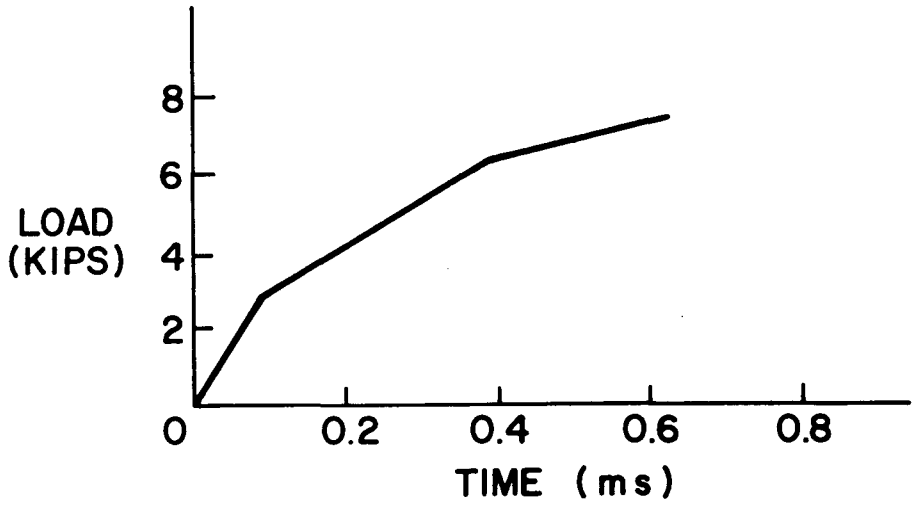

Assuming that the beam is initially acting as a single lumped mass system the differential equation of dynamic equilibrium can be written using D'Alembert's principle.

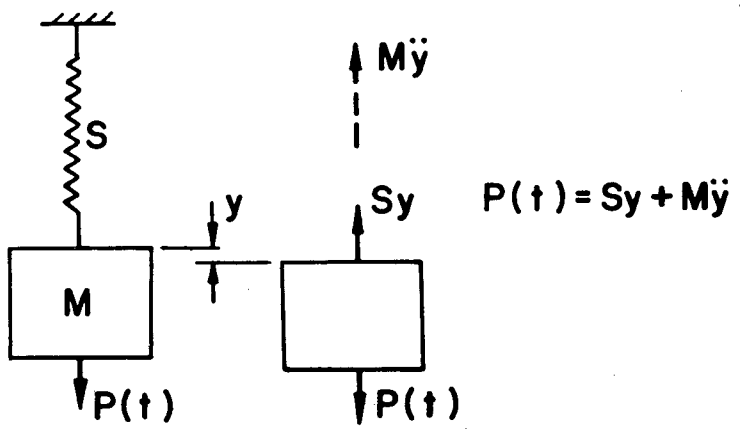

where

S = specimen stiffness

M = specimen mass

P(t) = loading function

y = specimen deflection at midspan

$\ddot{y}$ = specimen acceleration at midspan

After rearranging terms and inserting values the final equation of motion becomes

$$\ddot{y} = 77.3\ P(t) - (598 \times 10^5)\ y$$

Due to the complexity of the loading function a numerical integration procedure was used with an integration interval on the time axis of 1/10 of the natural period of the specimen

$$\Delta t = 0.030 \text{ ms}$$

The results of this step by step procedure are shown below along with the load that the specimen actually felt.

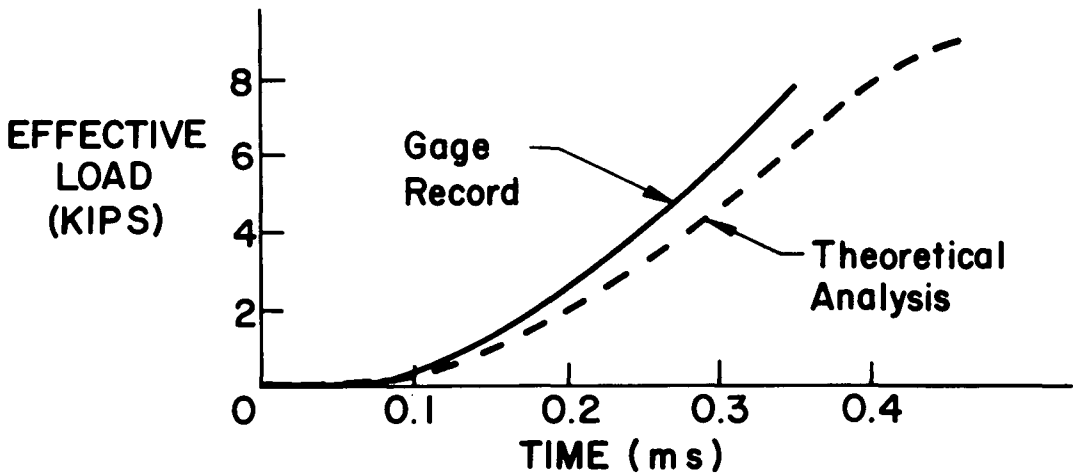

The experimental record and the theoretical curve are in close agreement indicating that a simple dynamic analysis of the single mass system can approximately describe specimen response during the loading cycle. This is based on the condition that the correct stiffness value of the specimen containing a crack can be determined.

The difference between the two curves could be due to the 1 inch overhang on either end of the specimen and the distributed mass of the system. Verification of these facts involves the dynamic analysis of a plate subjected to edge loading. Since this feature was not of primary interest in the project it was not investigated.

The results of this report are based on the fact that the tup records what the specimen actually feels. Comparison of the tup load at fracture and the load indicated by the beam gages substantiate this fact.

1. Tup Load

   $P = 7.50$ kips

2. Beam Gages on Specimen

   $P = 7.92$ kips

The fact that these loads are out of phase by a determinable amount was explained in Sec. 7.3.

It can be concluded from this comparison that the aluminum pad spreads out the loading time to the point where a quasi-static analysis can be used for the dynamic measurement of K_C.

TABLES AND FIGURES

TABLE 1: MATERIAL PROPERTIES OF 1/2 INCH PLATE

Heat No. 482T0241

Mechanical Properties*

Rolling Direction	Yield Strength** (ksi)	Ultimate Strength (ksi)	% Elongation	% Reduction in Area
Transverse	57.2	82.8	26.6	50.2
Longitudinal	56.7	83.1	27.2	61.5

Chemical Properties

C	Mn	P	S	Si	Cu	Cr	Ni	Mo	V
.20	1.08	.017	.025	.21	.23	.03	.02	.002	.051

*Determined from tests conducted at Fritz Engineering Laboratory.

**Loading Rate: from 0 to σ_Y in 50 seconds.

TABLE 2 TESTING SCHEDULE

Test Temperature (°F)	With Pad	Without Pad
-90	1/2" Diameter Aluminum Half Round 4' Drop Height	6" Drop Height
-40	1/2" Diameter Aluminum Half Round 4' Drop Height	1' Drop Height
0	1/2" Diameter Aluminum Half Round 4' Drop Height	1' Drop Height
+30	3/8" Diameter Aluminum Half Round 4' Drop Height	Invalid Test

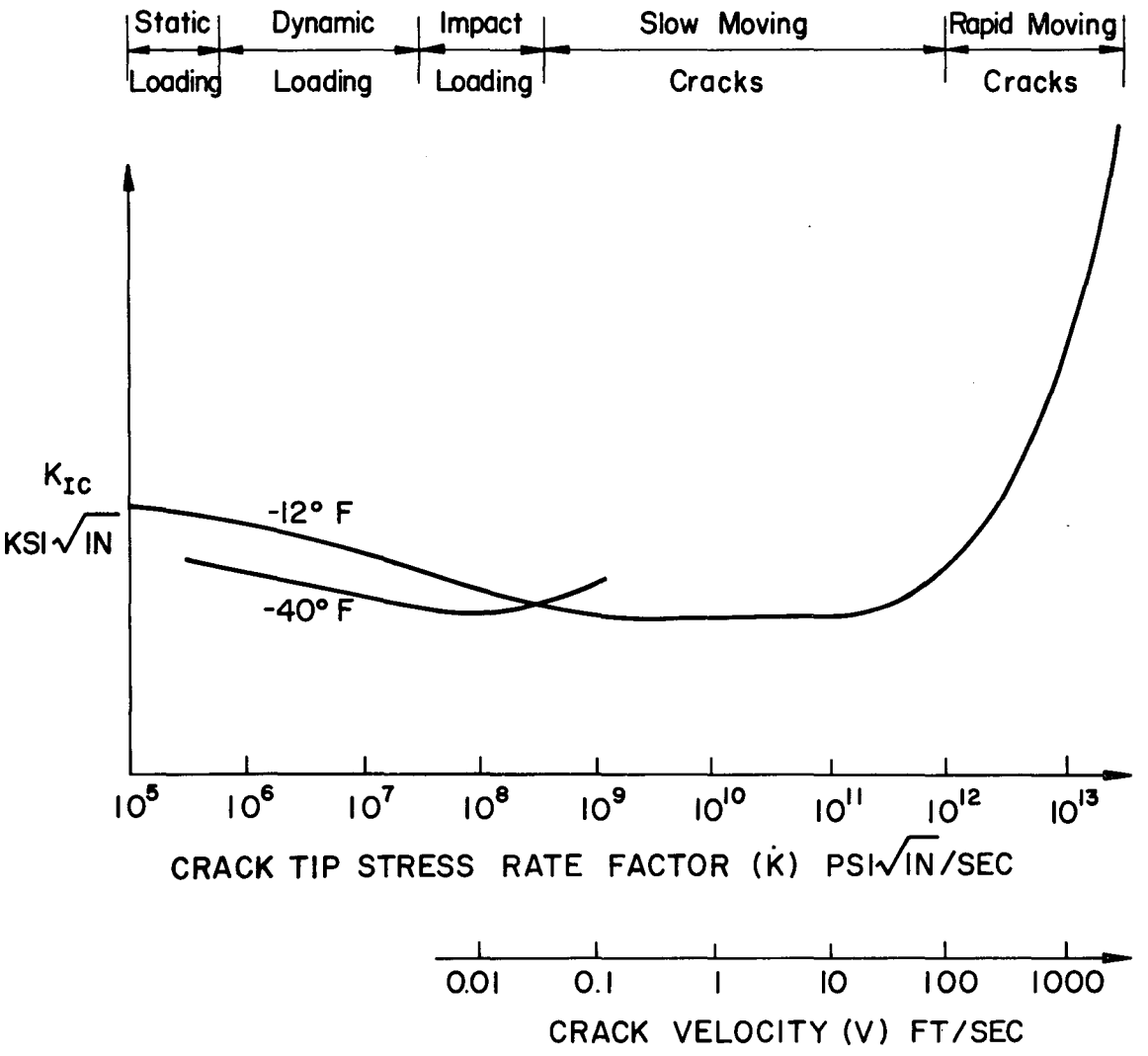

Fig. 1 VARIATION OF K_{IC} WITH CRACK TIP STRESS RATE

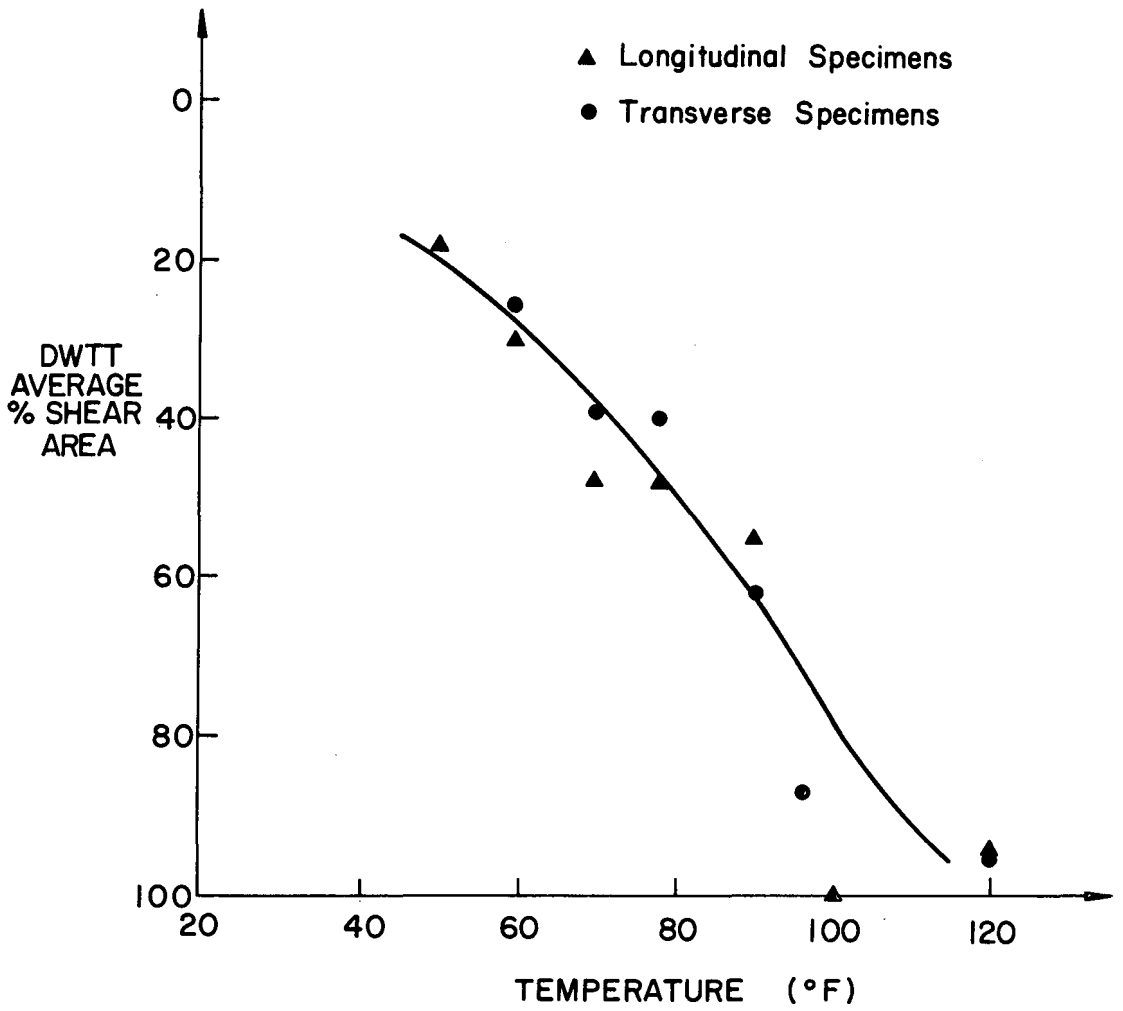

Fig. 2 PERCENTAGE SHEAR AREA VS. TEST TEMPERATURE - BATTELLE DROP WEIGHT TEAR TEST

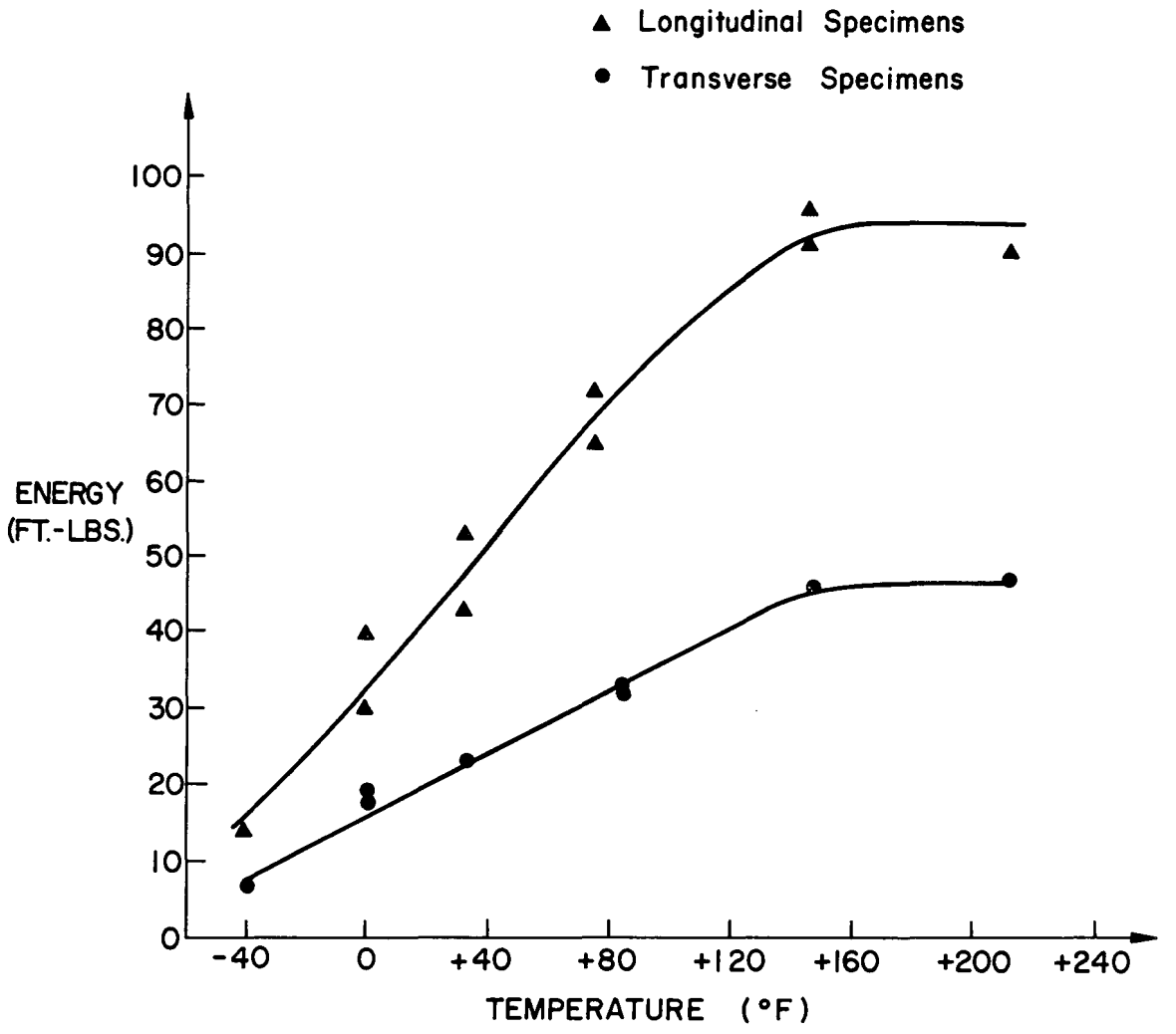

Fig. 3 FRACTURE ENERGY VS. TEST TEMPERATURE - CHARPY V NOTCH TEST

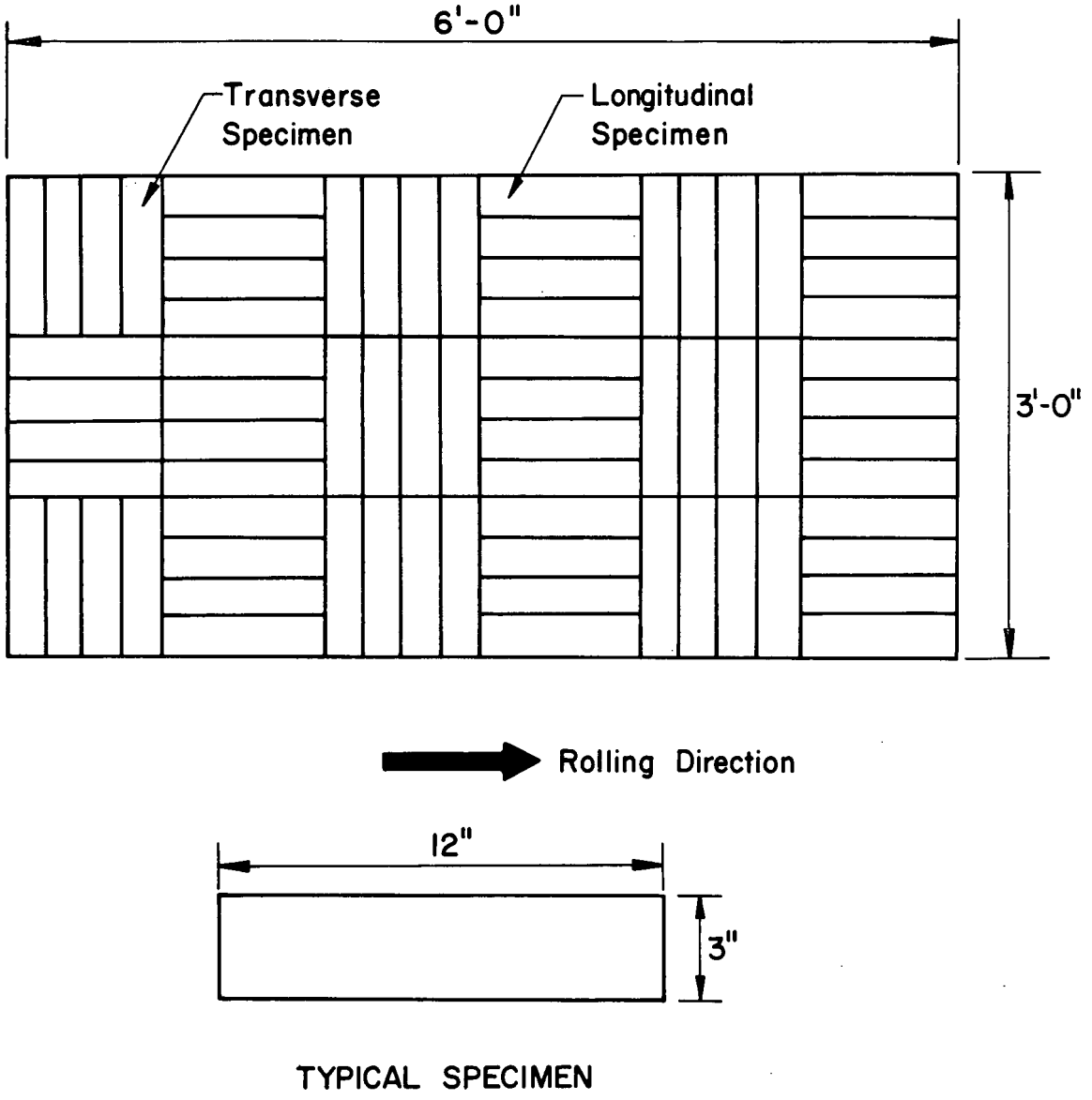

Fig. 4 SPECIMEN ORIENTATION IN ROLLED PLATE

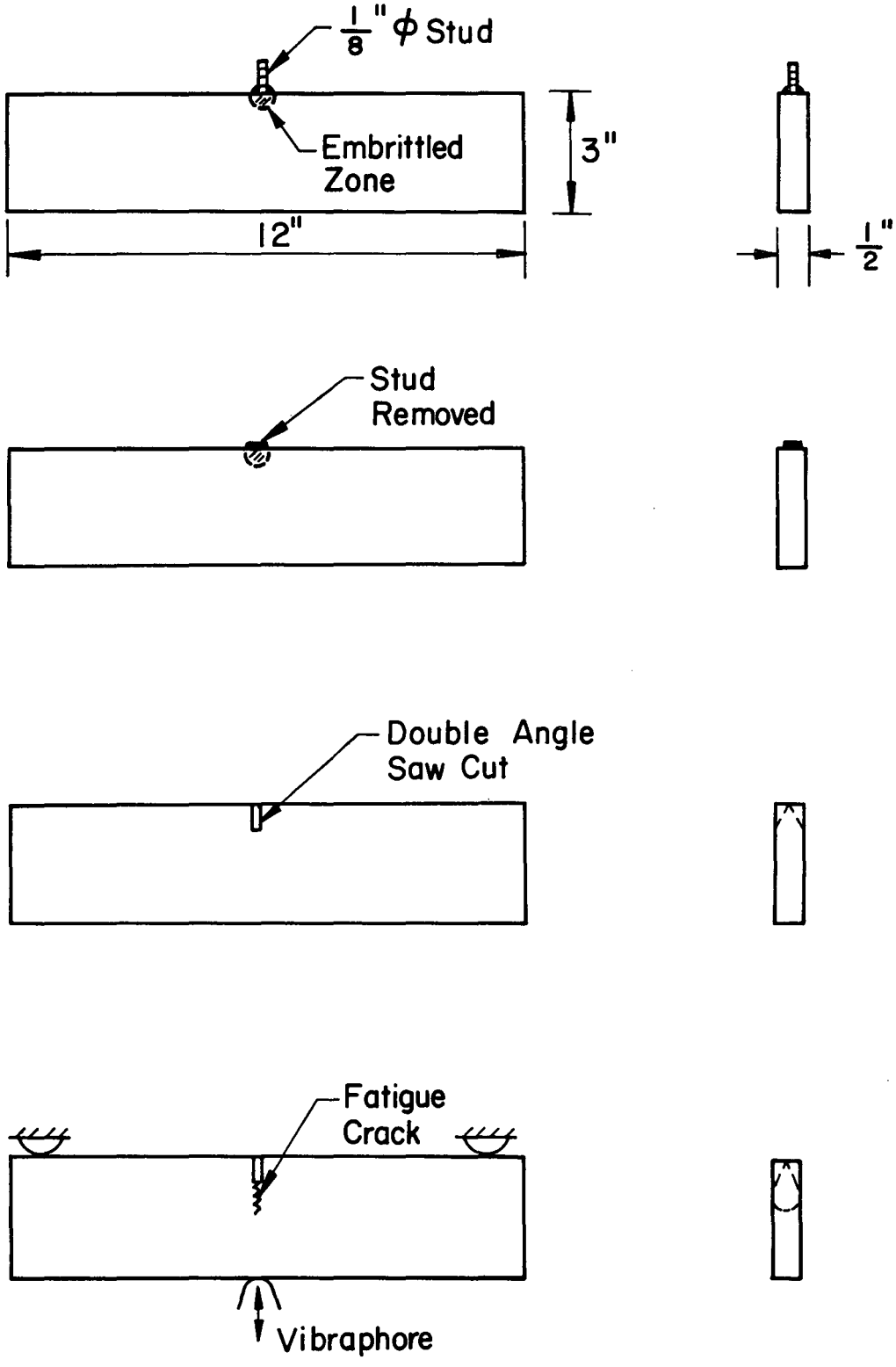

Fig. 5 STEPS IN FATIGUE CRACK INITIATION

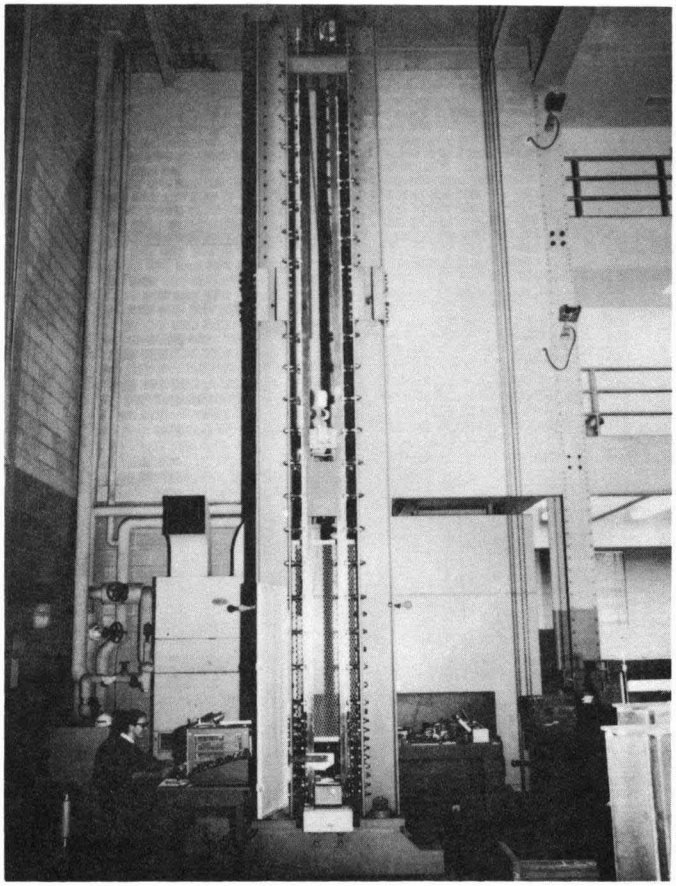

Fig. 6 DROP WEIGHT TEAR TESTING MACHINE

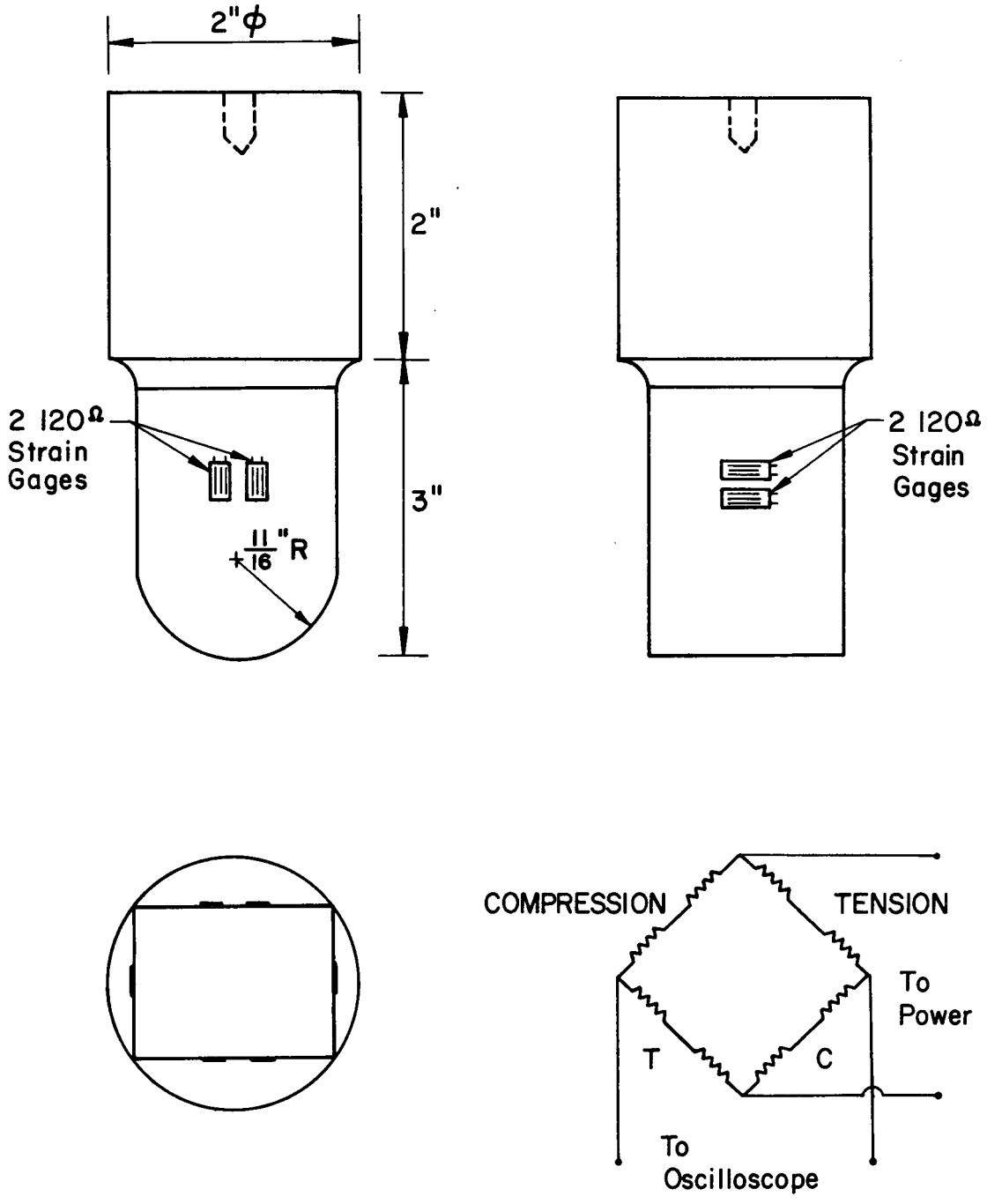

Fig. 7 LOAD RECORDING DYNAMOMETER (TUP)

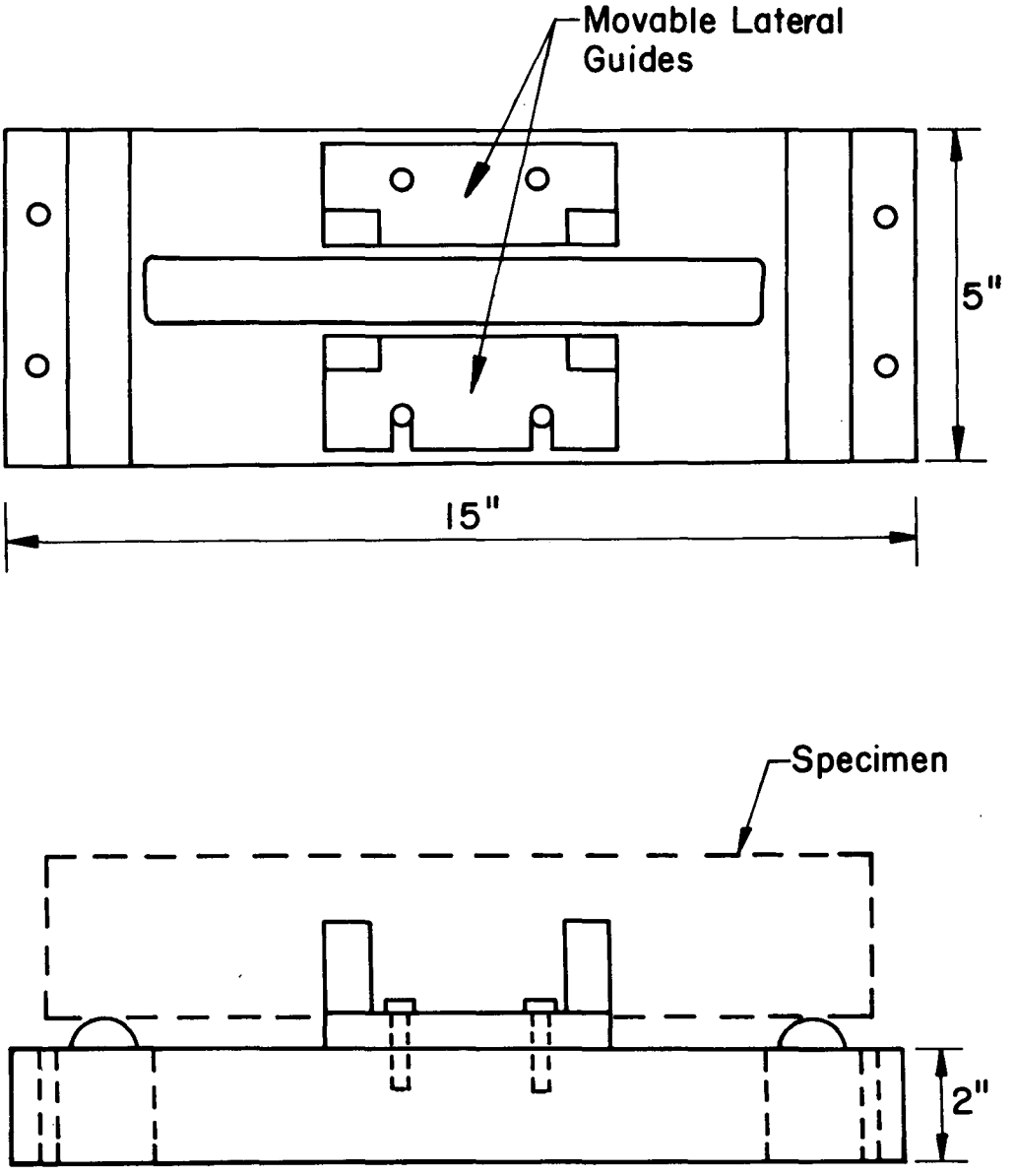

Fig. 8 TEST FIXTURE

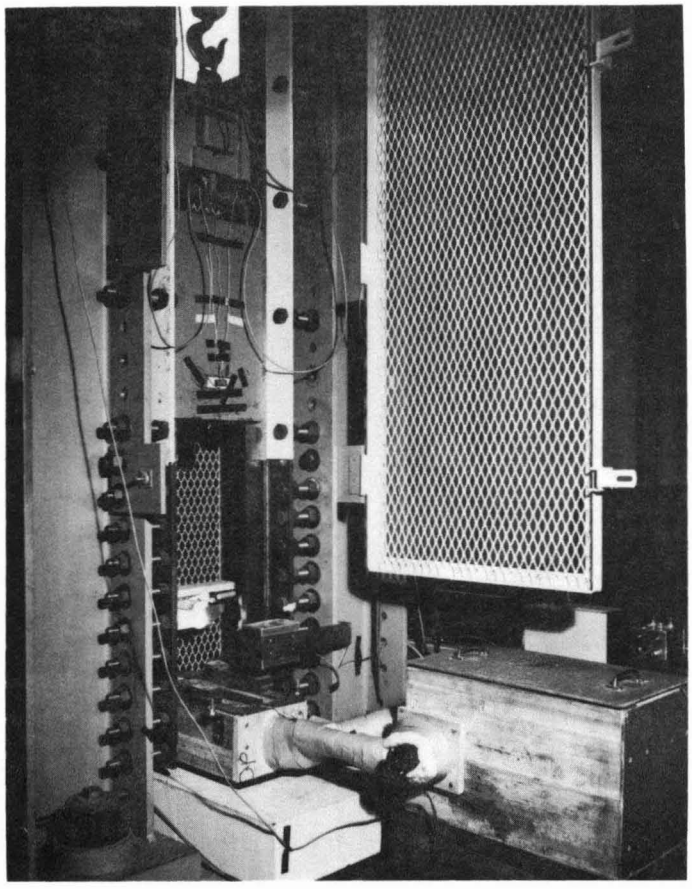

Fig. 9 COOLING SYSTEM

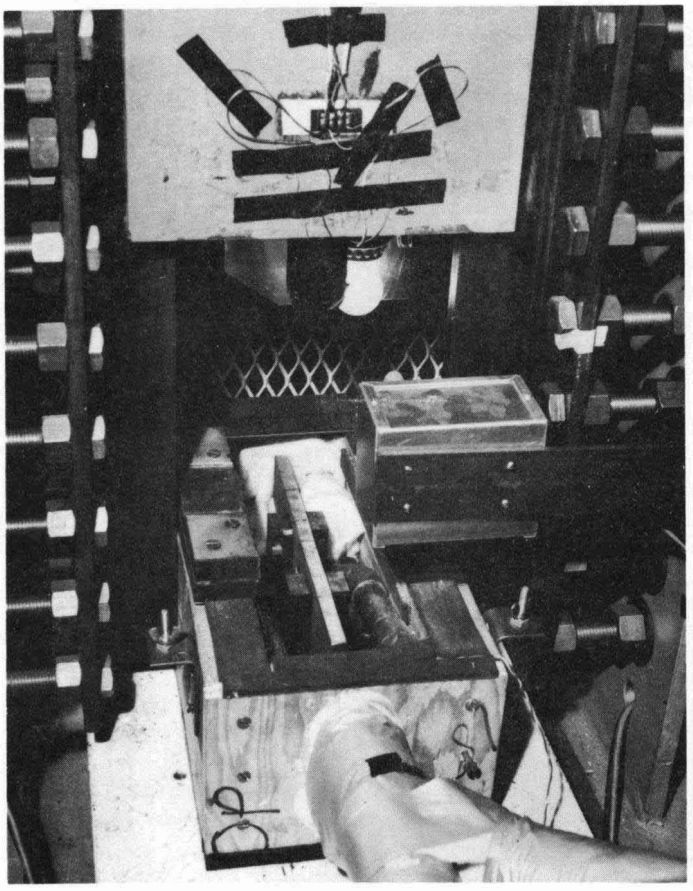

Fig. 10 SPECIMEN IN TEST FIXTURE

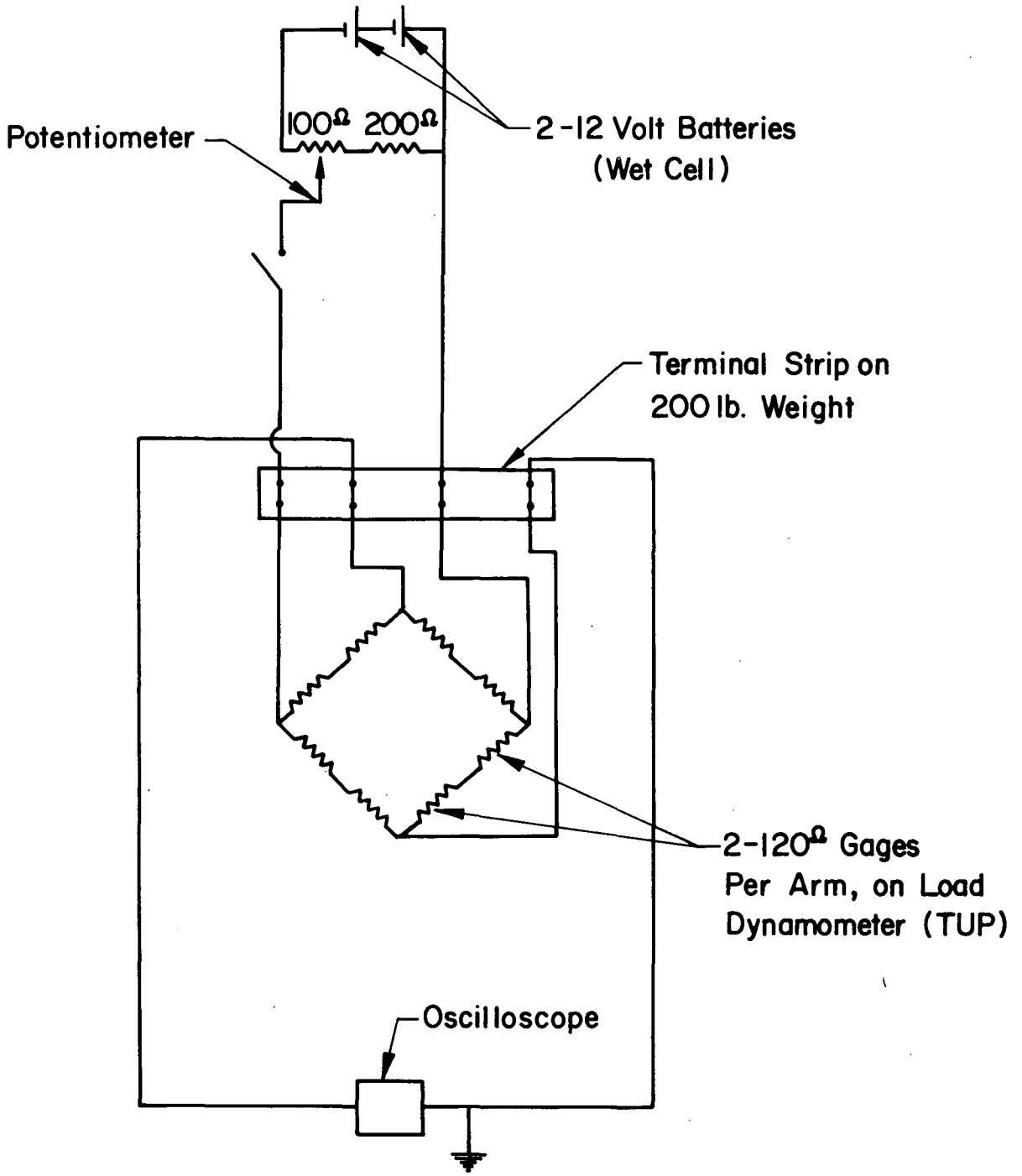

Fig. 11 ELECTRICAL CIRCUIT FOR LOAD RECORD

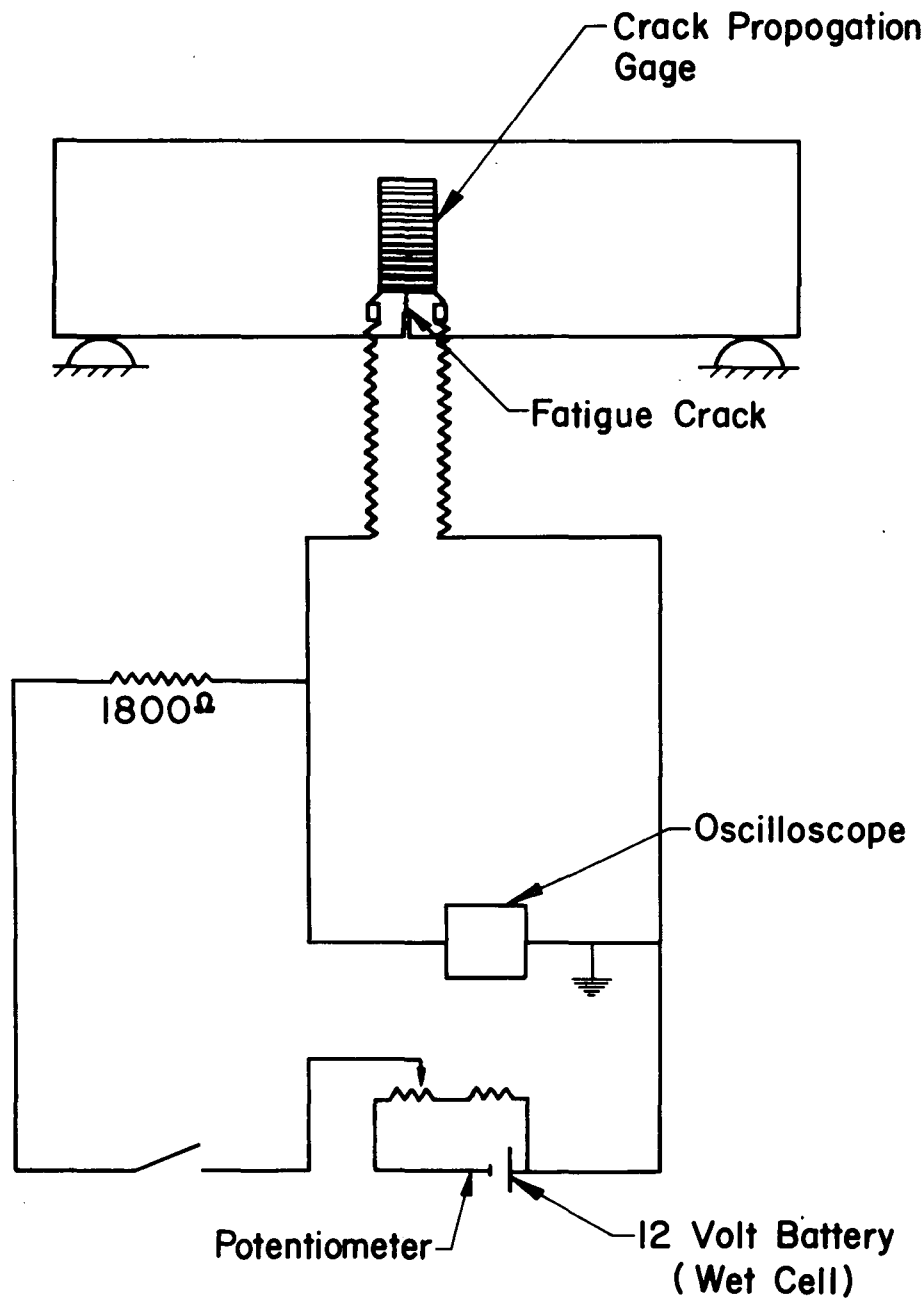

Fig. 12 ELECTRICAL CIRCUIT FOR CRACK PROPOGATION GAGE

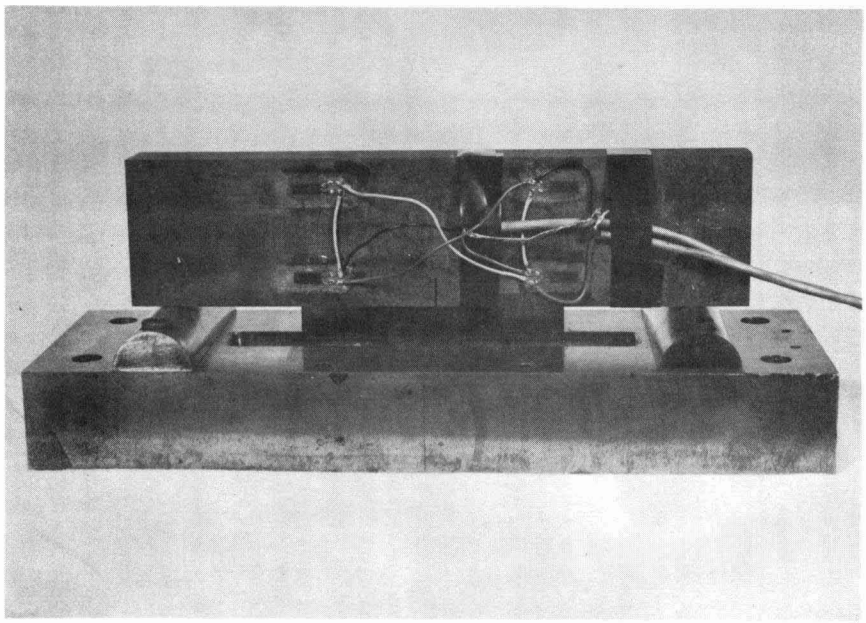

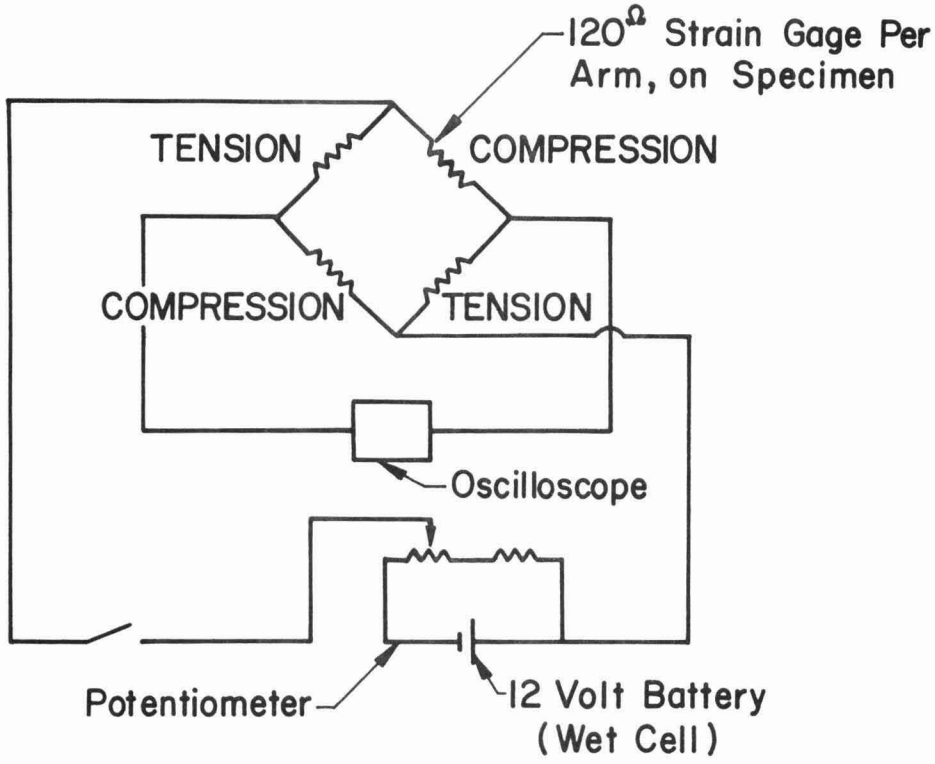

Fig. 13 ELECTRICAL CIRCUIT FOR GAGED BEND SPECIMEN

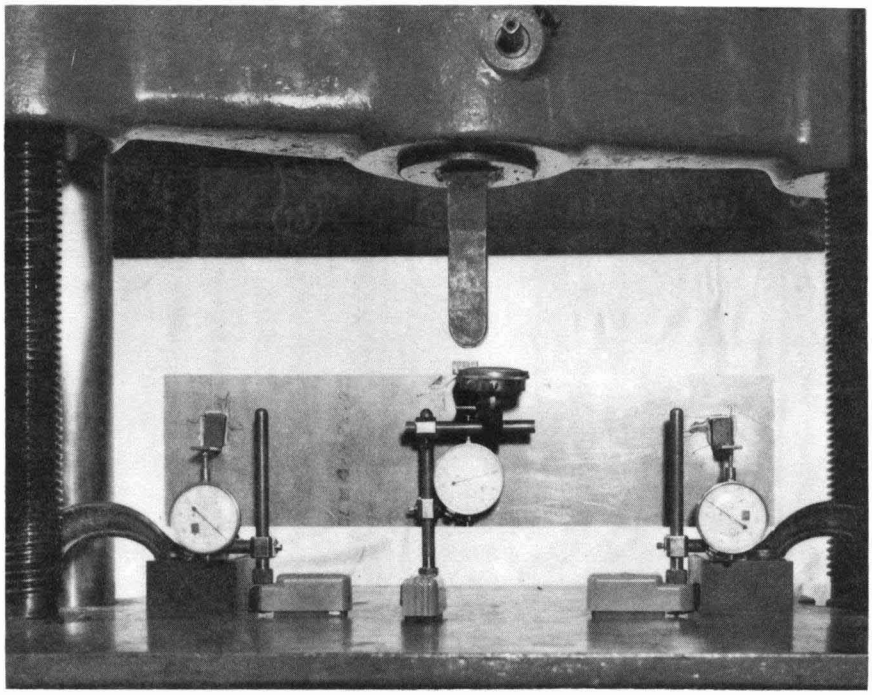

Fig. 14 COMPLIANCE CALIBRATION SPECIMEN

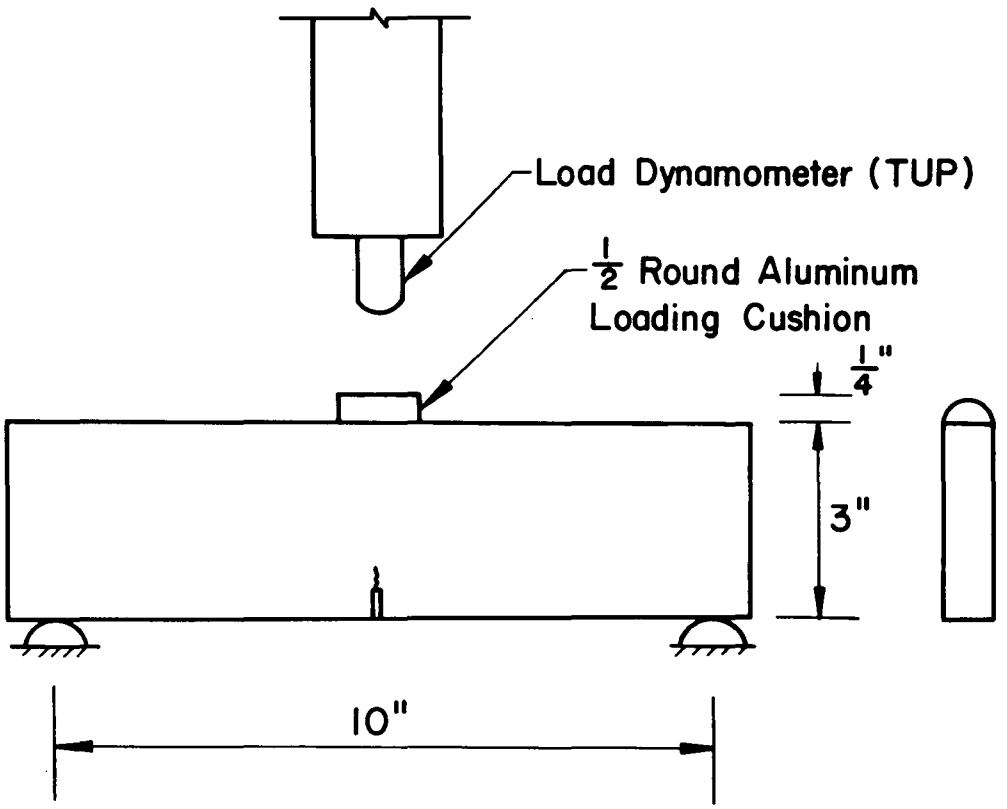

Fig. 15 PADDED SPECIMEN WITH ALUMINUM LOADING CUSHION

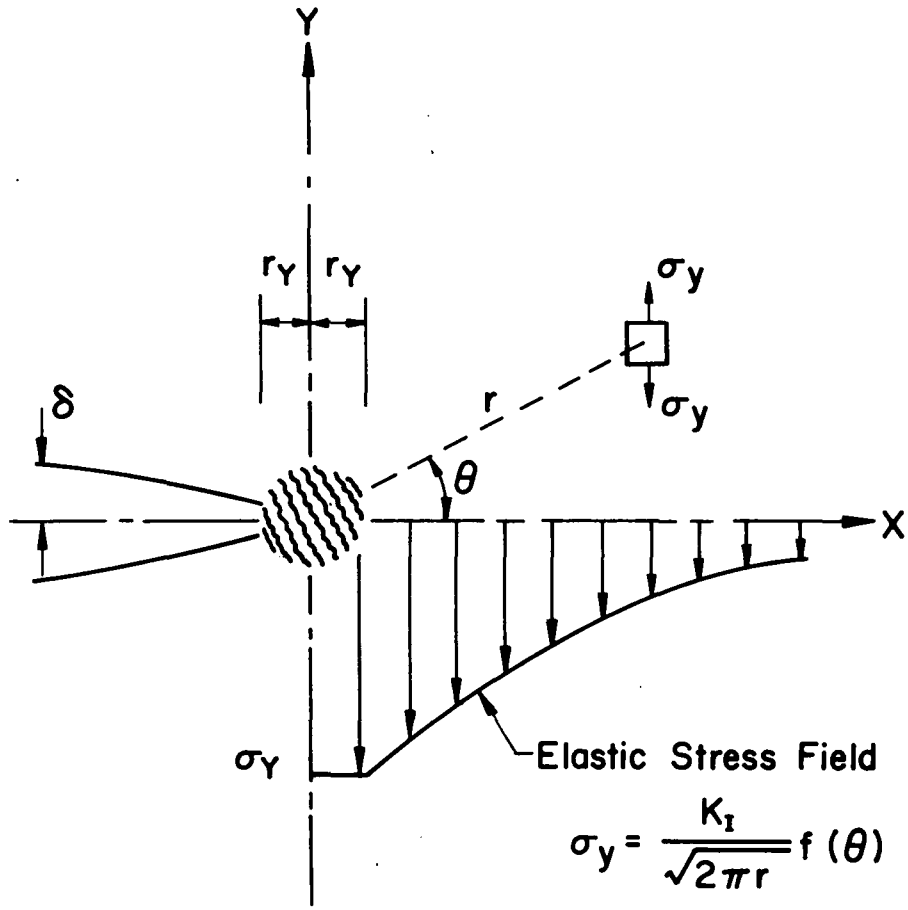

Where:

K_I = Stress Intensity Factor

δ = Crack Opening Displacement

E = Young's Modulus

μ = Poisson's Ratio

r_Y = Plastic Zone Adjustment

σ_Y = Yield Strength

Fig. 16 LEADING EDGE OF A CRACK

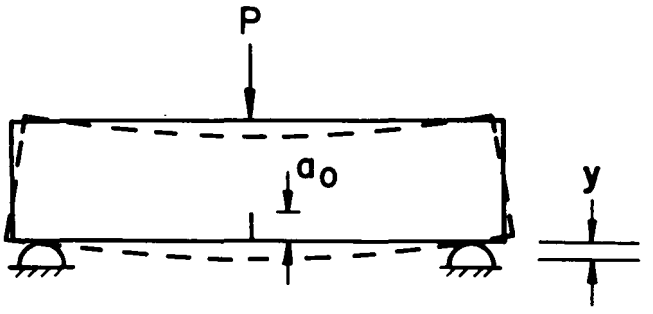

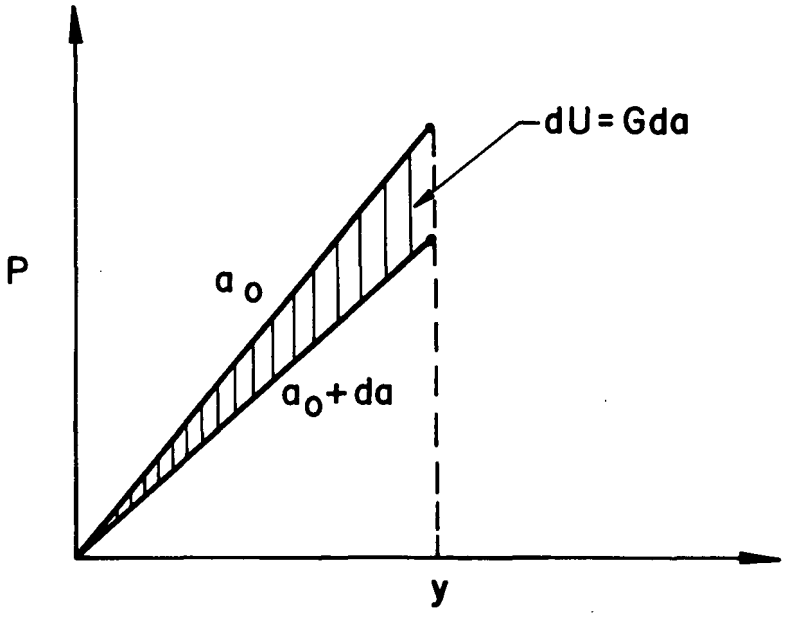

Fig. 17 LOAD VS. DEFORMATION CURVE FOR COMPLIANCE MEASUREMENT

$$Y = \frac{K_I BW^2}{1.5 PL\sqrt{a}}$$

$$= A_0 + A_1 \left(\frac{a}{W}\right) + A_2 \left(\frac{a}{W}\right)^2 + A_3 \left(\frac{a}{W}\right)^3 + A_4 \left(\frac{a}{W}\right)^4$$

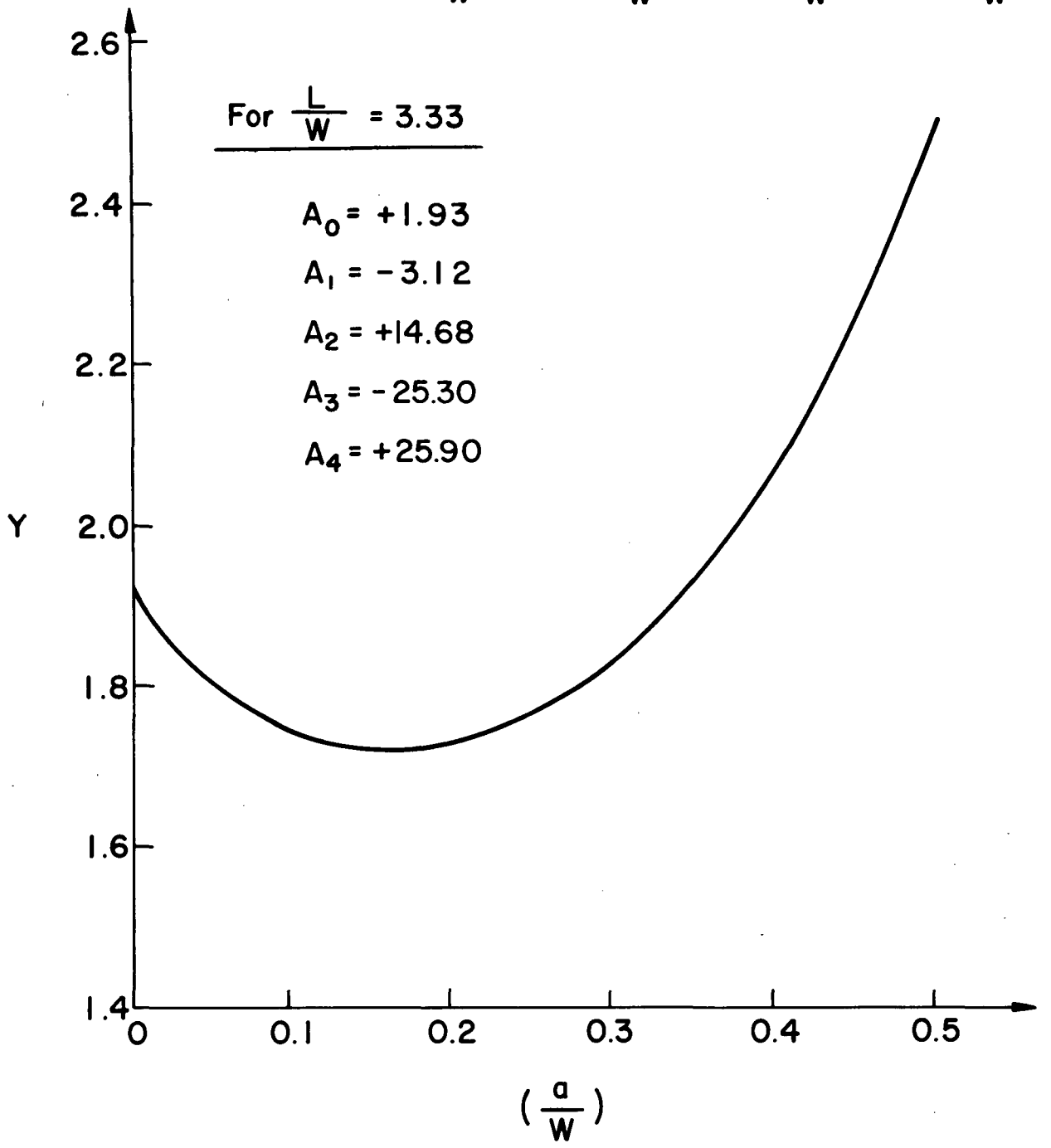

Fig. 18 CALIBRATION CURVE FOR BEND SPECIMEN WITH AN L/W RATIO OF 3.33

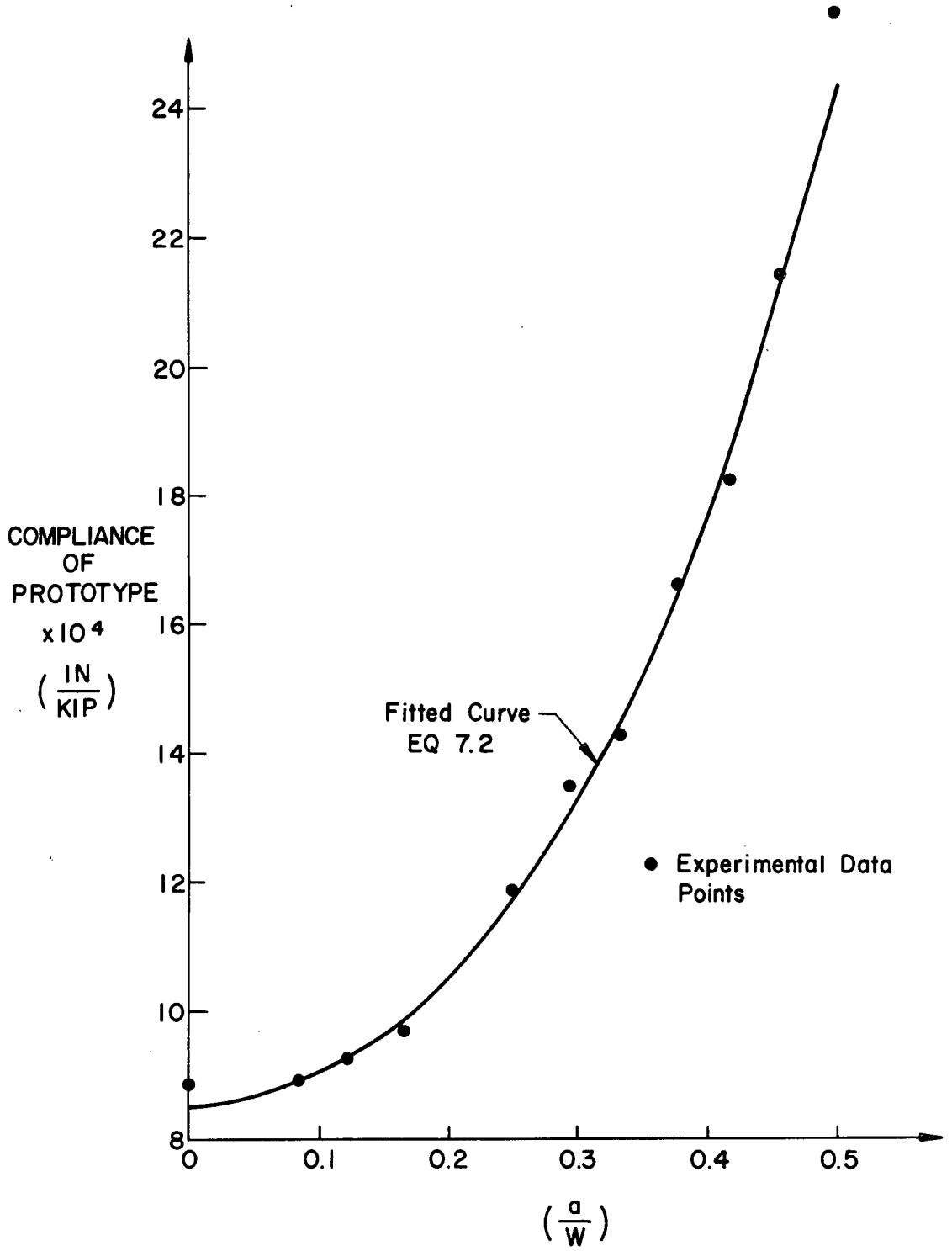

Fig. 19 PROTOTYPE COMPLIANCE VS. (a/W)

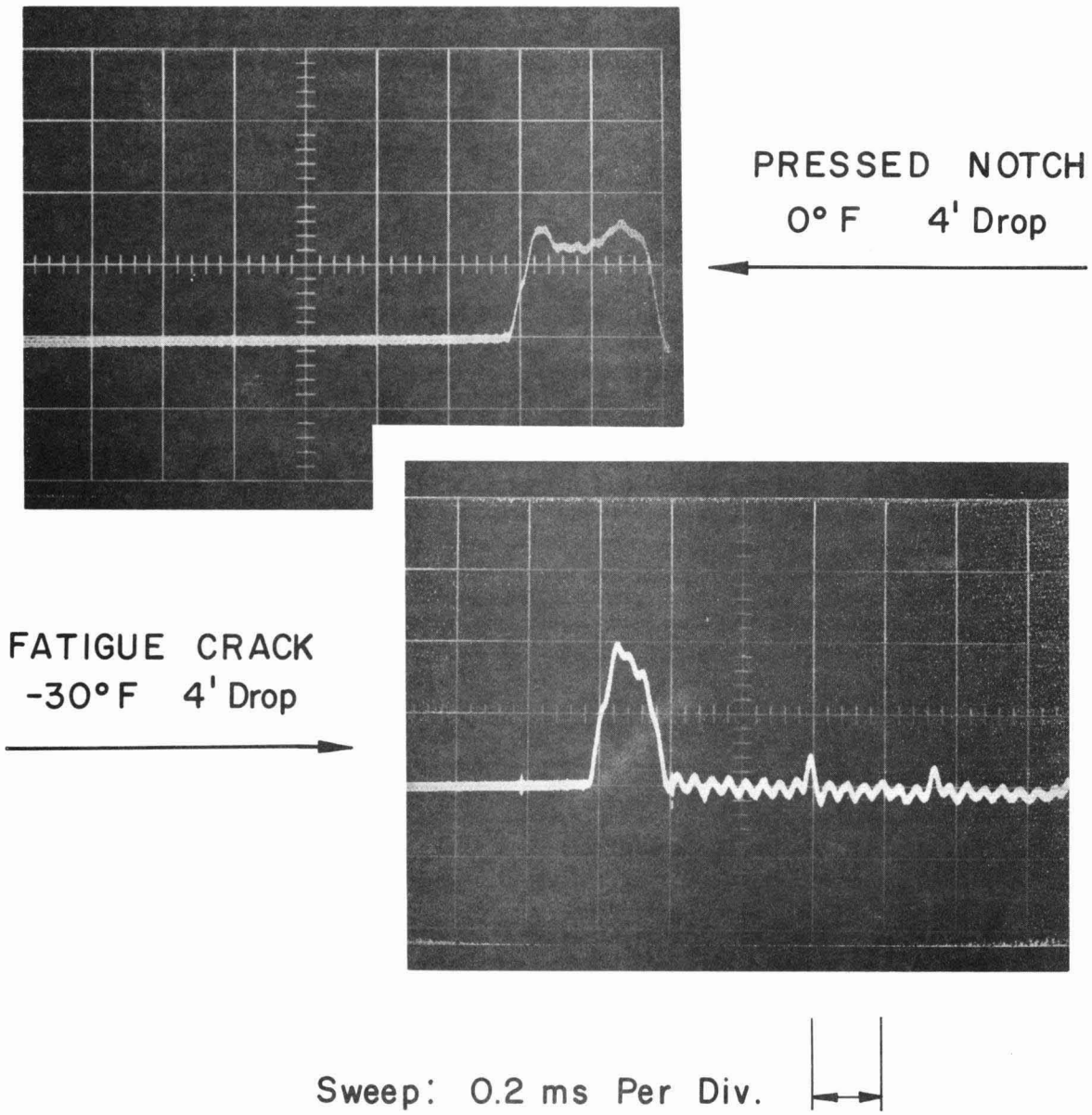

Fig. 20 LOAD RECORDS FOR A PRESSED NOTCH AND A FATIGUE CRACKED SPECIMEN

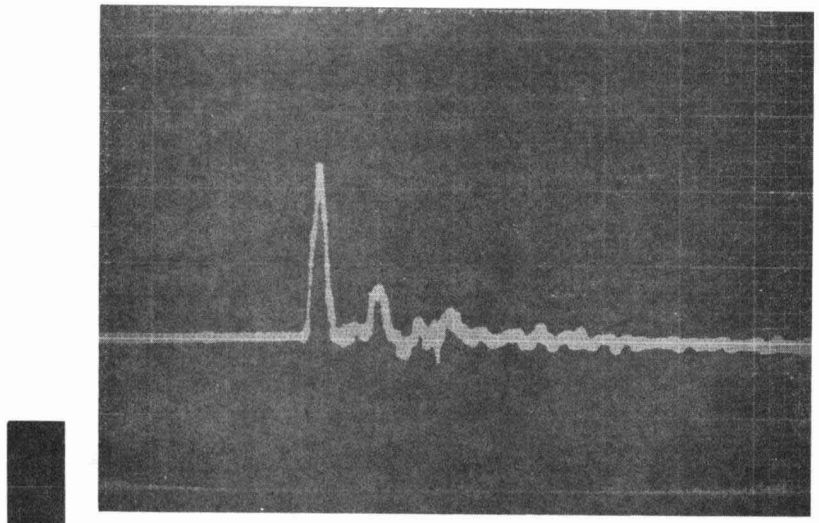

4' DROP
-16° F

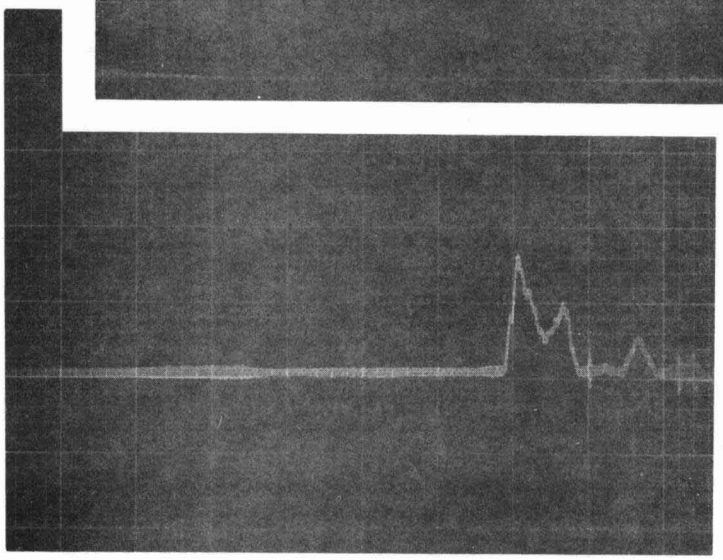

2' DROP
-25° F

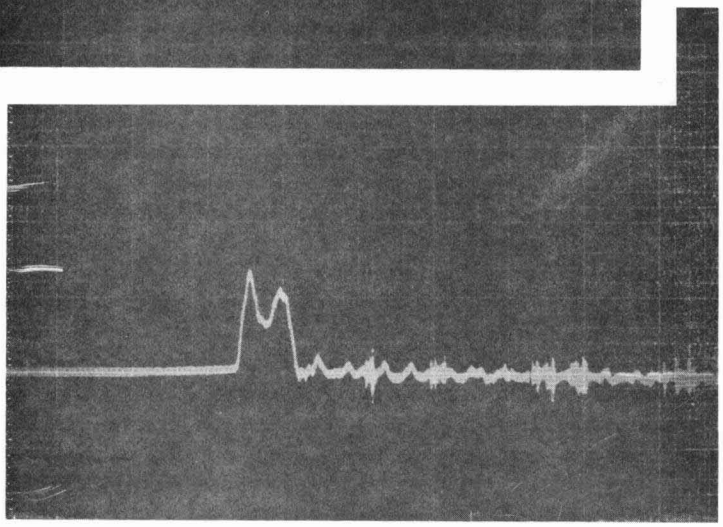

1' DROP
-44° F

Sweep: 0.5 ms Per Div.

Vertical Scale: 10 kips Per Div.

Fig. 21 LOAD RECORDS FOR VARIOUS DROP HEIGHTS

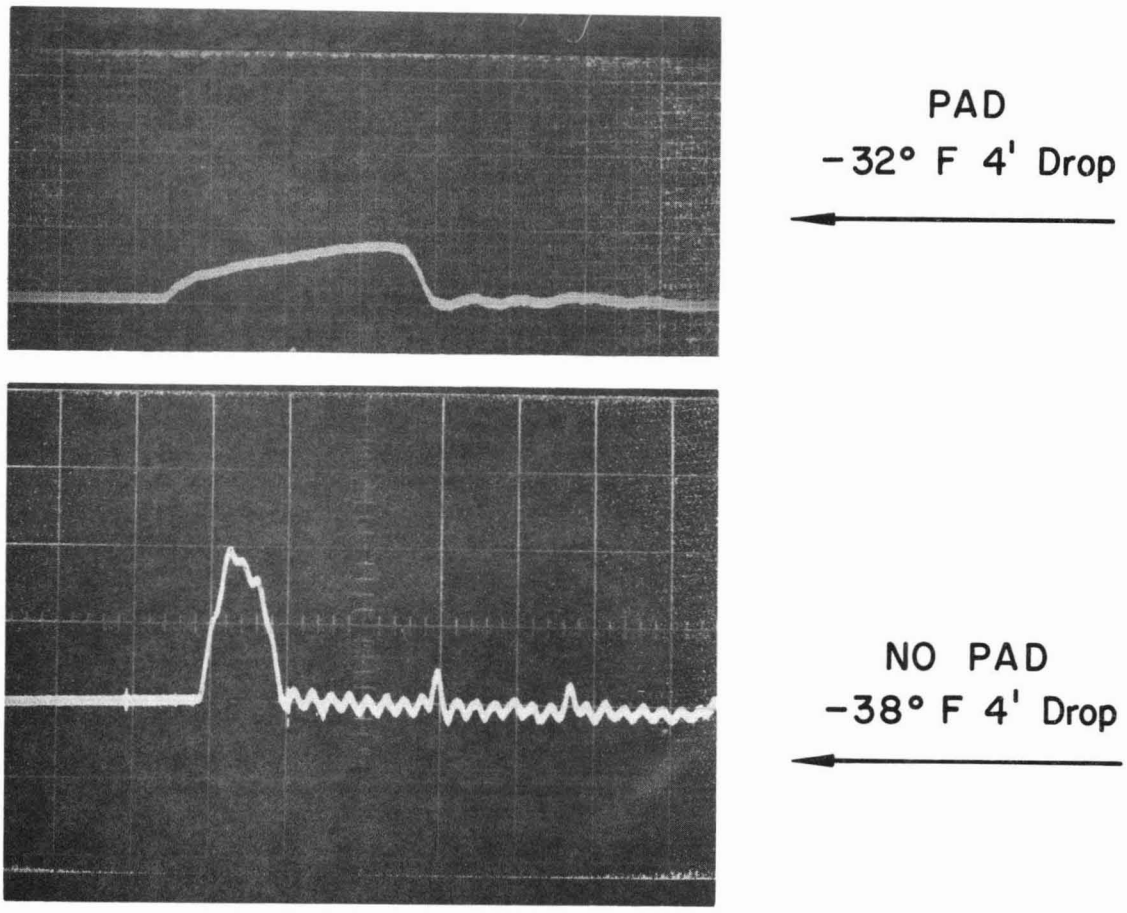

Fig. 22 LOAD RECORDS FOR A PADDED AND AN UNPADDED SPECIMEN

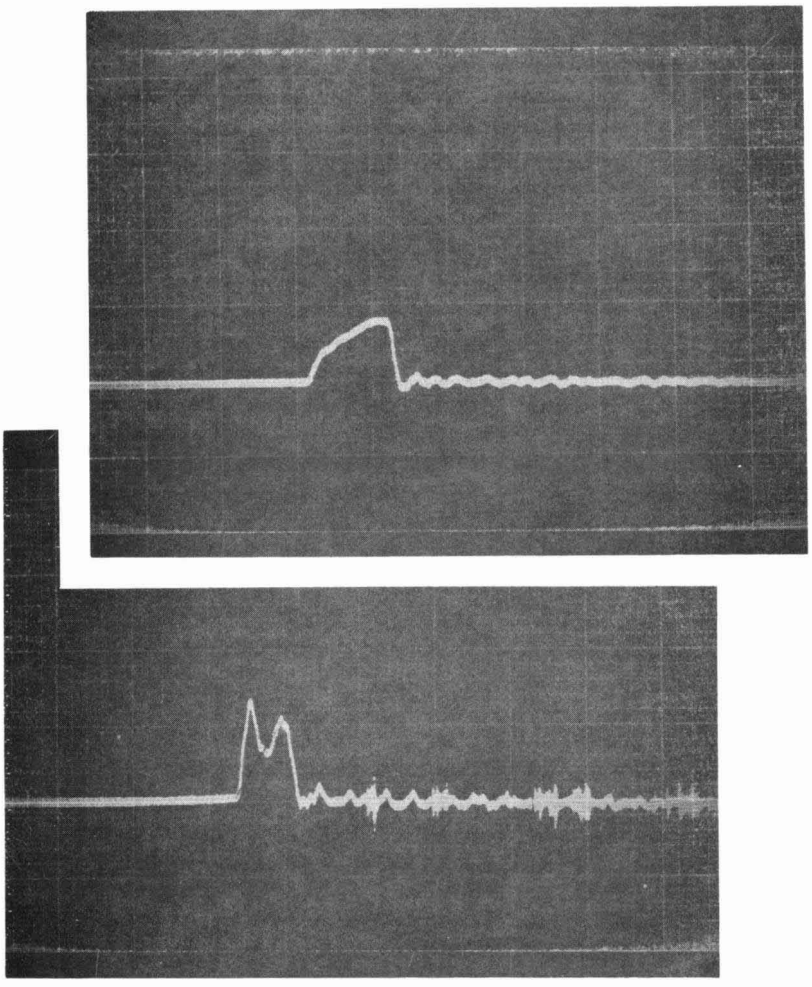

Fig. 23 TYPICAL LOAD RECORDS FOR K_C AND K_{IC} COMPUTATION

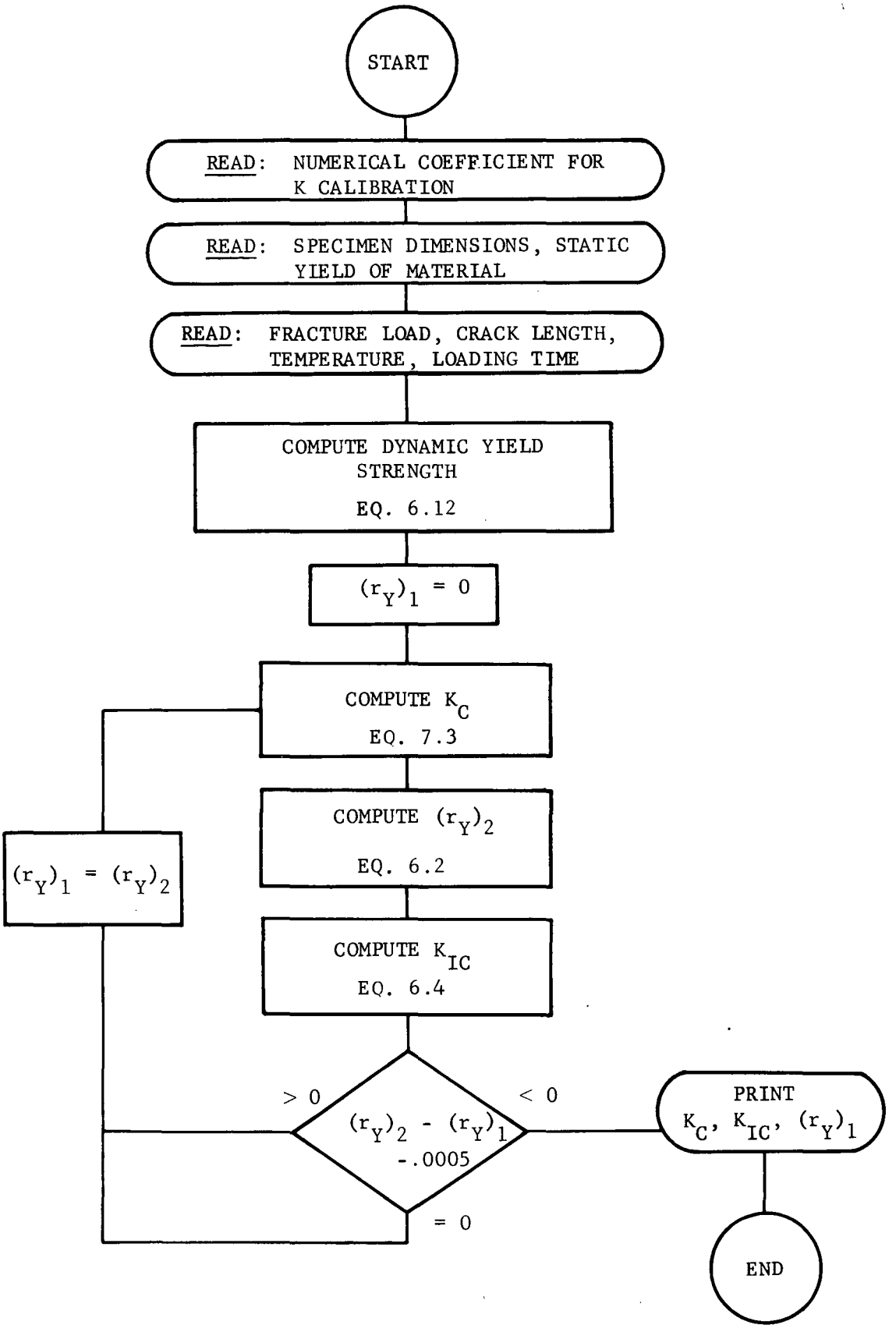

Fig. 24 FLOW CHART FOR K_C AND K_{IC} COMPUTATION

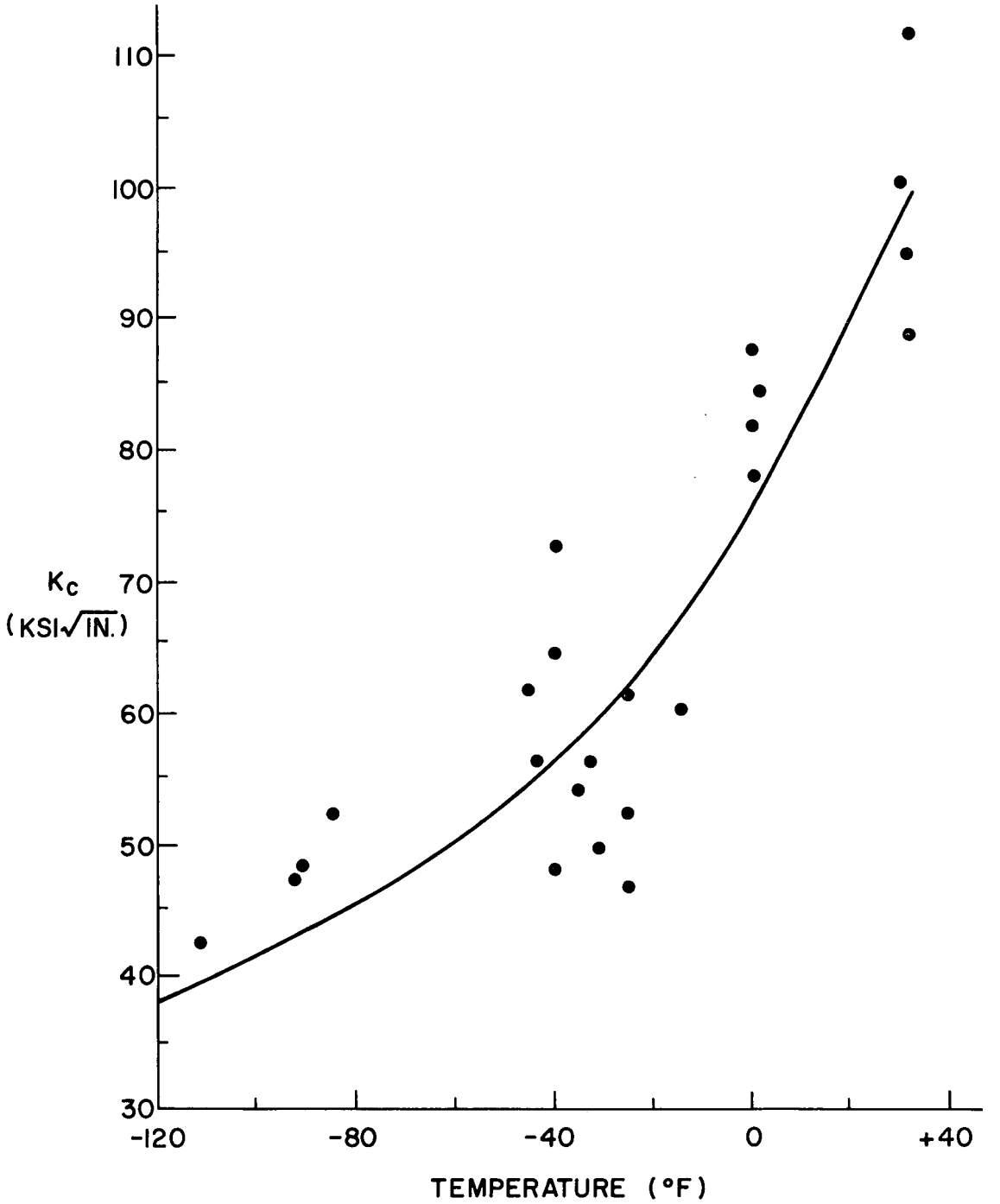

Fig. 25 K_C VS. TEMPERATURE

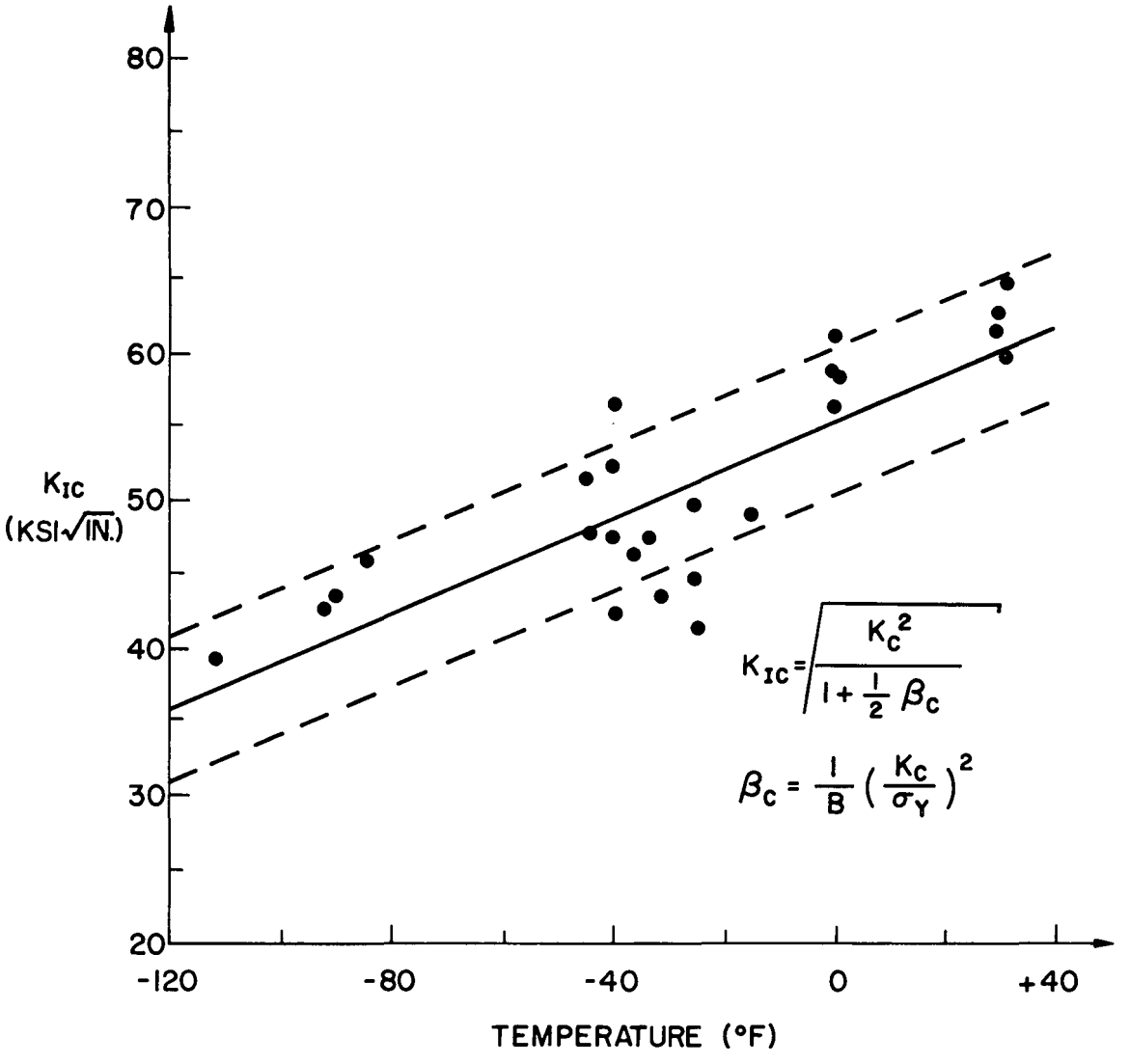

Fig. 26 K_{IC} VS. TEMPERATURE

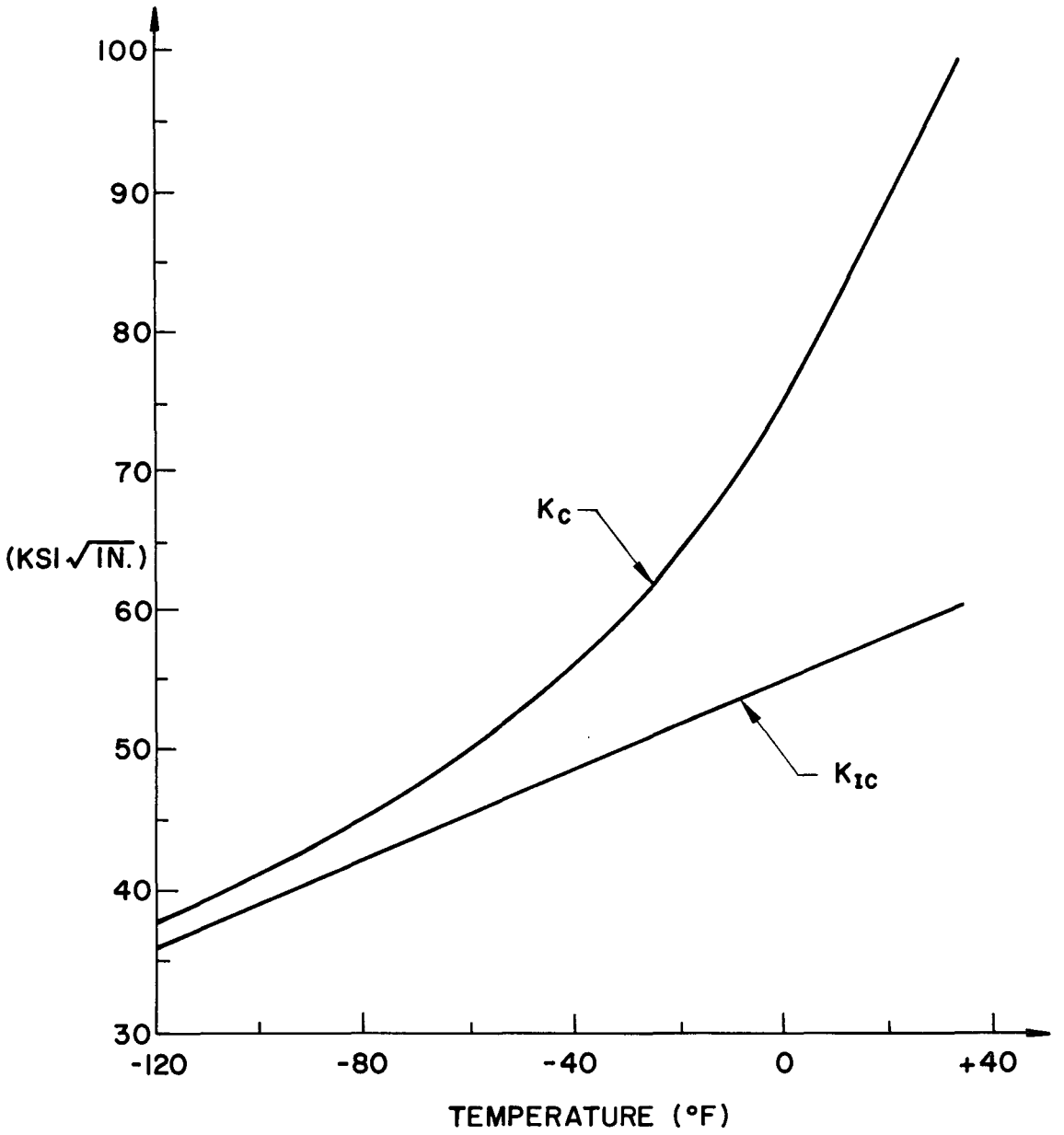

Fig. 27 COMPARISON OF K_C AND K_{IC} VARYING WITH TEMPERATURE

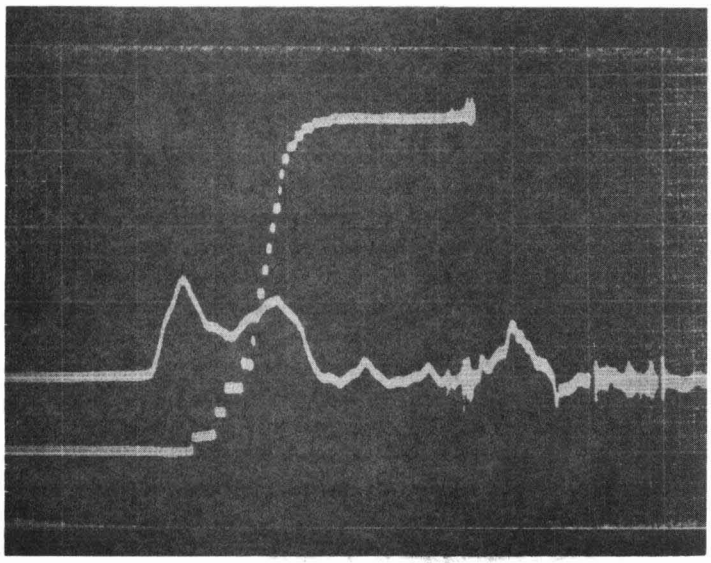

T = - 34° F

1' Drop

K_C = 54.0 ksi$\sqrt{in.}$

K_{IC} = 46.0 ksi$\sqrt{in.}$

Maximum Crack Speed = 1000 ft./sec.

Sweep: 0.2 ms Per Div.

(a) FATIGUE CRACK

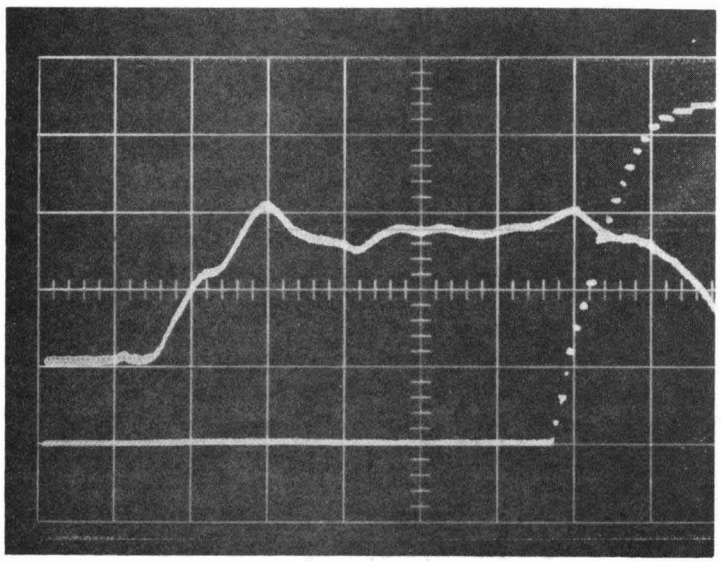

T = 0° F

7' Drop

K_C = 60.1 ksi$\sqrt{in.}$

K_{IC} = 49.2 ksi$\sqrt{in.}$

Maximum Crack Speed = 2100 ft./sec.

Sweep: 0.05 ms Per Div.

(b) PRESSED NOTCH

Fig. 28 COMPARISON OF CRACK WIRE RECORDS FOR A FATIGUE CRACK AND FOR A PRESSED NOTCH

T = − 32° F
4' Drop
Pad

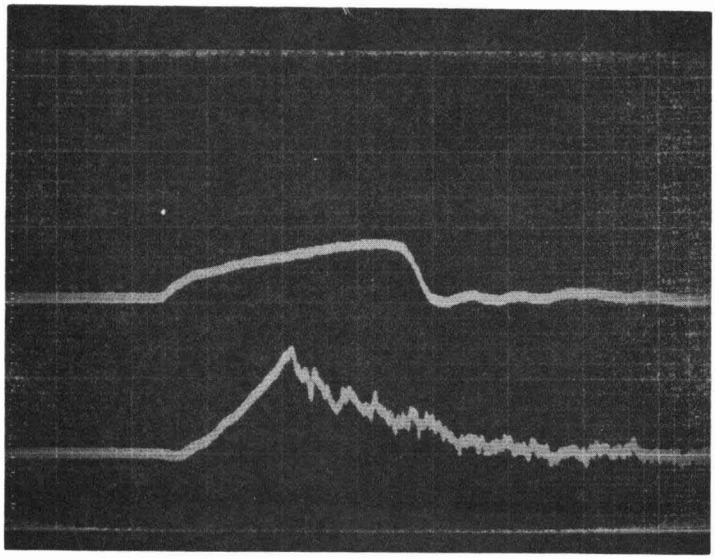

TUP GAGES
K_c = 49.6 ksi$\sqrt{in.}$
BEAM GAGES
K_c = 53.2 ksi$\sqrt{in.}$

Sweep: 0.2 ms Per Div.

Upper Trace Vertical Scale: 10 kips Per Div.

Lower Trace Vertical Scale: 5.92 kips Per Div.

Fig. 29 COMPARISON OF LOAD RECORD AND BENDING STRAIN RECORD

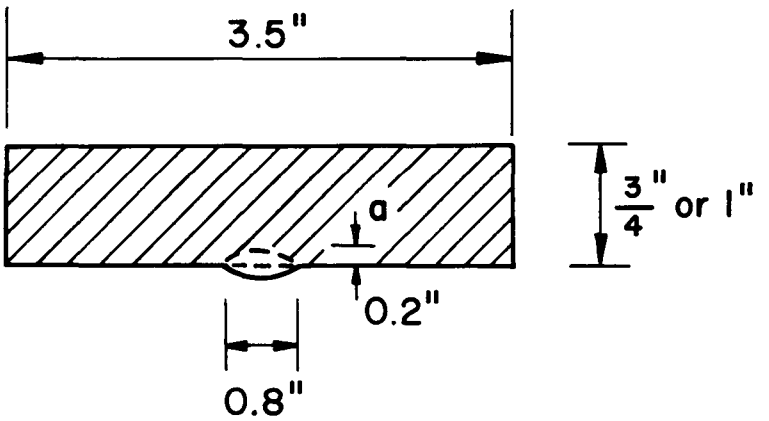

$$K^2 = \frac{1.2\,\pi\,a\,\sigma^2}{\phi^2 - 0.212\left(\frac{\sigma}{\sigma_Y}\right)^2}$$

AT NDT: $K_{Id} = 0.78\,\sqrt{IN.}\cdot\sigma_{Yd}$

Fig. 30 FRACTURE SECTION OF NDT SPECIMEN

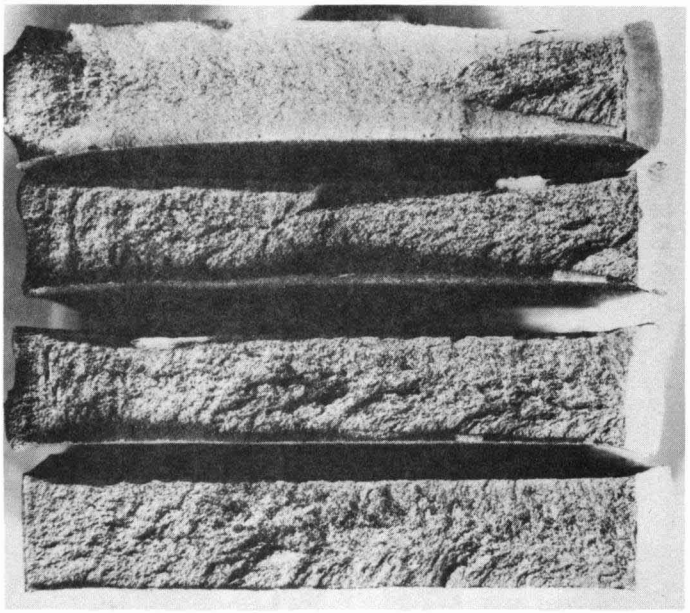

TEMPERATURE
+120° F
+80° F
+50° F
+0° F

(a) PRESSED NOTCH

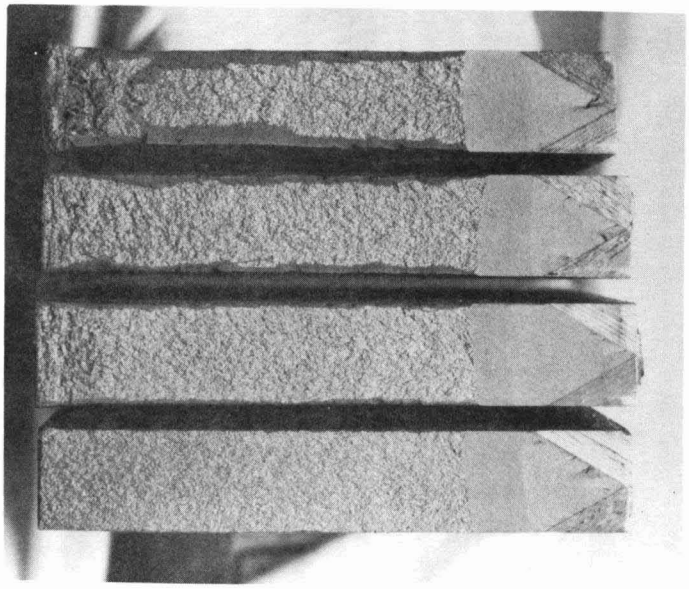

TEMP.	K_c KSI$\sqrt{IN.}$
+30° F	88.6
+0° F	77.9
−30° F	56.2
−90° F	47.2

(b) FATIGUE CRACK

Fig. 31 FRACTURE SURFACES

REFERENCES

1. Brown, Jr., W. F. and J. E. Srawley
PLANE STRAIN CRACK TOUGHNESS TESTING OF HIGH STRENGTH METALLIC MATERIALS,
ASTM STP410, Philadelphia, 1966

2. ASTM Specifications
HIGH STRENGTH LOW ALLOY STRUCTURAL MANGANESE VANADIUM STEEL,
ASTM Specification No. A441-66a, Vol. 4, 1968

3. ASTM Specifications
NOTCHED BAR IMPACT TESTING OF METALLIC MATERIALS,
ASTM Specification No. E24-64, Vol. 30, 1966

4. ASTM Specifications
DROP WEIGHT TEST TO DETERMINE NIL DUCTILITY TRANSITION TEMPERATURE OF FERRITIC STEELS,
ASTM Specification No. E208066T, Vol. 30, 1967

5. Pellini, W. S. and P. P. Puzak
FACTORS THAT DETERMINE THE APPLICABILITY OF HIGH STRENGTH QUENCHED AND TEMPERED STEEL TO SUBMARINE HULL CONSTRUCTION,
NRL Report 5892, December 5, 1962

6. Eiber, R. J. and G. M. McClure
LABORATORY FRACTURE TESTS - THEIR RELATION TO FULL SCALE PROPERTIES,
Oil and Gas Journal, September 23, 1963

7. Griffith, A. A.
PHENOMENA OF RUPTURE AND FLOW IN SOLIDS,
Philosophical Transaction of the Royal Society of London, Vol. 221, pp. 163-198, October 21, 1920

8. Irwin, G. R.
FRACTURE DYNAMICS,
Symposium Vol. "Fracturing of Metals", pp. 147-166,
ASTM (Cleveland) 1948

9. Orowan, E.
FUNDAMENTALS OF BRITTLE BEHAVIOR OF METALS,
Symposium on Fatigue and Fracture of Metals,
John Wiley & Son, Inc., New York, p. 139, 1952

REFERENCES (continued)

10. Shoemaker, A. K. and S. T. Rolfe
STATIC AND DYNAMIC LOW TEMPERATURE K_{IC} BEHAVIOR OF STEELS,
U. S. Steel Applied Research Laboratory, Project No. 39.018-007(16)
(available from the Defense Documentation Centre)

11. Krafft, J. M. and G. R. Irwin
CRACK VELOCITY CONSIDERATIONS,
Fracture Toughness Testing and Its Application,
ASTM STP381, 1965

12. Gross, B. and J. E. Srawley
STRESS INTENSITY FACTORS FOR THREE POINT BEND SPECIMENS BY BOUNDARY COLLOCATION,
Technical Note D-3092, NASA, December 1965

13. Irwin, G. R. and J. A. Kies
CRITICAL ENERGY RATE ANALYSIS OF FRACTURE STRENGTH,
Welding Journal, Research Supplement, Vol. 33, p. 193s, April, 1954

14. Irwin, G. R., J. A. Kies and H. L. Smith
FRACTURE STRENGTH RELATIVE TO ONSET AND ARREST OF CRACK PROPOGATION,
Proc. ASTM, Vol. 58, pp. 640-660, 1958

15. Kies, J. A., H. L. Smith, H. E. Romine and H. Bernstein
FRACTURE TESTING OF WELDMENTS,
Fracture Toughness Testing and Its Applications,
ASTM STP381, p. 328, 1965

16. Krafft, J. M.
TECHNIQUES OF MATERIALS RESEARCH,
Vol. 5, Chapter 7, 1st edition, Wiley Interscience
(not yet published)

17. Irwin, G. R.
ANALYSIS OF STRESSES AND STRAINS NEAR THE END OF A CRACK TRAVERSING A PLATE,
Trans. ASME, Journal of Applied Mechanics, Vol. 24, p. 361, 1957

18. Irwin, G. R.
PLASTIC ZONE NEAR A CRACK AND FRACTURE TOUGHNESS,
7th Sagamore Ordnance Materials Research Conference,
Proc. published by Syracuse University, 1961

REFERENCES (continued)

19. Special ASTM Committee
FRACTURE TESTING OF HIGH STRENGTH SHEET MATERIALS,
ASTM Bulletin No. 243, p. 29, 1960

20. Irwin, G. R.
FRACTURE MODE TRANSITION FOR A CRACK TRAVERSING A PLATE,
Trans. ASME, Vol. 82, No. 2, p. 417, 1960

21. Irwin, G. R.
STRUCTURAL ASPECTS OF BRITTLE FRACTURE,
Applied Materials Research, Vol. 3, p. 65, April 1964

22. Irwin G. R.
LECTURE NOTES IN MECHANICS 350 (Fracture Mechanics),
Lehigh University, Fall Semester, 1967

23. Wessel, E. T., W. G. Clark, and W. K. Wilson
ENGINEERING METHODS FOR THE DESIGN AND SELECTION OF MATERIALS AGAINST FRACTURE,
Westinghouse Research Laboratory Report to Army Tank-Automotive Centre, June 24, 1966

24. Irwin, G. R.
LINEAR FRACTURE MECHANICS, FRACTURE TRANSITION, AND FRACTURE CONTROL,
Journal of Engineering Fracture Mechanics,
Vol. 1, No. 2, 1968

25. Yoffe, E. H.
THE MOVING GRIFFITH CRACK,
Philosophical Magazine, Vol. 42, p. 739, 1951

26. Irwin, G. R., J. M. Krafft, P. C. Paris, and A. A. Wells
BASIC ASPECTS OF CRACK GROWTH AND FRACTURE,
NRL Report 6598, November 21, 1967

27. Biggs, J. M.
INTRODUCTION TO STRUCTURAL DYNAMICS,
1st Edition, McGraw-Hill, New York, 1964